JACS
JOURNAL OF THE AMERICAN CHEMICAL SOCIETY
Article
pubs.acs.org/JACS

Reduction of CO_2 to Methanol Catalyzed by a Biomimetic Organo-Hydride Produced from Pyridine

Chern-Hooi Lim,[†] Aaron M. Holder,[†,‡] James T. Hynes,[‡,§] and Charles B. Musgrave*[,†,‡]

[†]Department of Chemical and Biological Engineering and [‡]Department of Chemistry and Biochemistry, University of Colorado, Boulder, Colorado 80309, United States

[§]Chemistry Department, Ecole Normale Supérieure, UMR ENS-CNRS-UPMC 8640, 24 rue Lhomond, 75005 Paris, France

Supporting Information

ABSTRACT: We use quantum chemical calculations to elucidate a viable mechanism for pyridine-catalyzed reduction of CO_2 to methanol involving homogeneous catalytic steps. The first phase of the catalytic cycle involves generation of the key catalytic agent, 1,2-dihydropyridine (**PyH_2**). First, pyridine (Py) undergoes a H^+ transfer (PT) to form pyridinium (PyH^+), followed by an e^- transfer (ET) to produce pyridinium radical (PyH^0). Examples of systems to effect this ET to populate PyH^+'s LUMO ($E^0_{calc} \sim -1.3$ V vs SCE) to form the solution phase PyH^0 via highly reducing electrons include the photoelectrochemical p-GaP system ($E_{CBM} \sim -1.5$ V vs SCE at pH 5) and the photochemical $[Ru(phen)_3]^{2+}$/ascorbate system. We predict that PyH^0 undergoes further PT−ET steps to form the key closed-shell, dearomatized (**PyH_2**) species (with the PT capable of being assisted by a negatively biased cathode). Our proposed sequential PT−ET−PT−ET mechanism for transforming Py into **PyH_2** is analogous to that described in the formation of related dihydropyridines. Because it is driven by its proclivity to regain aromaticity, **PyH_2** is a potent recyclable organo-hydride donor that mimics important aspects of the role of NADPH in the formation of C−H bonds in the photosynthetic CO_2 reduction process. In particular, in the second phase of the catalytic cycle, which involves three separate reduction steps, we predict that the **PyH_2**/Py redox couple is kinetically and thermodynamically competent in catalytically effecting hydride and proton transfers (the latter often mediated by a proton relay chain) to CO_2 and its two succeeding intermediates, namely, formic acid and formaldehyde, to ultimately form CH_3OH. The hydride and proton transfers for the first of these reduction steps, the homogeneous reduction of CO_2, are sequential in nature (in which the formate to formic acid protonation can be assisted by a negatively biased cathode). In contrast, these transfers are coupled in each of the two subsequent homogeneous hydride and proton transfer steps to reduce formic acid and formaldehyde.

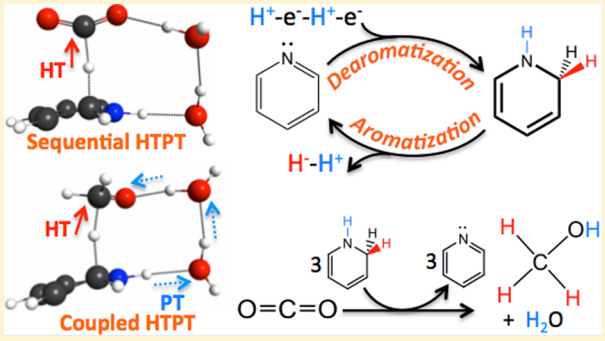

1. INTRODUCTION

Conversion of carbon dioxide (CO_2) to fuels enabling a closed-carbon cycle powered by renewable energy has the potential to dramatically impact the energy and environmental fields.[1−10] However, the chemical reduction of CO_2 to highly reduced products such as methanol (CH_3OH) remains a daunting task. The groups of Fujita,[11−13] Kubiak,[3,14] Meyer,[15−17] Savéant,[18−20] and others[21−32] have made significant contributions to this field, particularly in the fundamental understanding of using transition-metal complexes to catalyze CO_2's transformation. Despite these advances, many challenges remain: for example, CO_2 reduction has largely been confined to $2e^-$ products such as CO and formate, and, in many cases, large overpotentials are required to drive these reactions.[11,14,18,22]

Recently, Bocarsly and co-workers[23,33] employed pyridine (Py) in a photoelectrochemical system using a p-type GaP cathode to efficiently convert CO_2 to CH_3OH at 96% Faradaic efficiency and 300 mV of underpotential;[23] it is notable that although semiconductor cathodes, such as n-GaAs, p-GaAs, and p-InP, have been shown to convert CO_2 to CH_3OH without Py when biased to potentials more negative than −1 V vs SCE,[34,35] on a p-GaP cathode under illumination and biased to only ∼−0.2 V vs SCE,[23] CH_3OH is produced only in the presence of Py; thus, Py evidently plays a key role in catalyzing the formation of CH_3OH from CO_2. Clearly, a thorough understanding of any Py-catalyzed CO_2 reduction is required not only to elucidate Py's catalytic role in general but also to develop related catalysts that exploit the fundamental phenomena at play in such a reduction. In this contribution, we use quantum chemical calculations to discover that the key to Py's catalytic behavior lies in the homogeneous chemistry of the 1,2-dihydropyridine/pyridine redox couple, driven by a dearomatization-aromatization process, in which 1,2-dihydropyridine (**PyH_2**) acts as a recyclable organo-hydride that reduces CO_2 to CH_3OH via three hydride and proton transfer (HTPT) steps (Scheme 1).

Received: October 1, 2014

   dx.doi.org/10.1021/ja510131a | J. Am. Chem. Soc. XXXX, XXX, XXX−XXX

Scheme 1. Homogeneous Reduction of CO_2 to Methanol by 1,2-Dihydropyridine via Hydride and Proton Transfer Steps

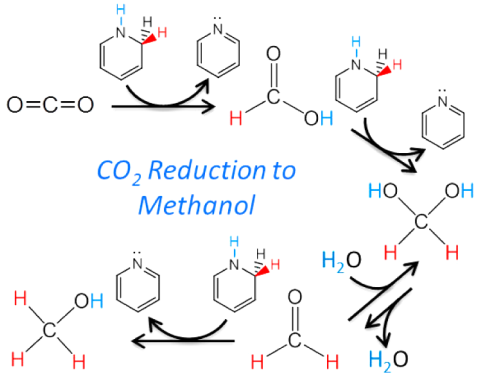

We pause to stress that while the fundamental reduction mechanism that we develop (the generation of **PyH_2** and three catalytic steps to reduce CO_2 progressively to CH_3OH) can operate under homogeneous conditions (although probably with low CH_3OH yield at typically employed pH values; *vide infra*), we do find that the mechanism can be assisted at two stages by the influence of the double layer adjoining the negatively biased cathode. These involve a step in the **PyH_2** formation and the formate−formic acid conversion preparatory to formic acid reduction. Even with these assisting heterogeneous aspects, the overall process is predominantly homogeneous and is active in their absence. We will use "homogeneous" as a descriptor for reaction steps where appropriate and will explicitly indicate the two junctures where cathode heterogeneous effects assist the mechanism.

Hydride transfer (HT) reactions, which are formally equivalent to $2e^-/H^+$ reductions, have proven to be adept in forming C−H bonds, converting CO_2 to CH_3OH under mild conditions.[24,28,31] For example, we have shown how ammonia borane (H_3N-BH_3)[36] accomplishes hydride (H^-) and proton (H^+) transfers to CO_2 that ultimately lead to CH_3OH.[37,38] The particular relevance of this example is that **PyH_2**, the hydride reagent of special focus in this article, is similar to ammonia borane in that both involve a protic hydrogen on N which has neighboring hydridic hydrogens: on the ortho-C of 1,2-dihydropyridine and on the B of ammonia borane. However, **PyH_2** is unique in the critical sense that it is a catalytic hydride donor (*vide infra*), similar to NADPH in photosynthesis (as discussed within), rather than a stoichiometric hydride reagent (such as ammonia borane and silanes).

The outline of the remainder of this article is as follows. Using quantum chemical calculations whose methodology is outlined in Section 2, we will: (1) demonstrate how Py is transformed into the recyclable organo-hydride **PyH_2**, via a sequential PT−ET−PT−ET process (Sections 3.1 and 3.2). **PyH_2** is a $2H^+/2e^-$ transfer product of pyridine (Py).[39−42] We note that the formation of related dihydropyridines proceeds via sequential PT and ET steps;[43−45] (2) establish the hydride nucleophilicity of **PyH_2** and related dihydropyridines (Section 3.3); (3) calculate key transition states and reaction free energies to demonstrate that **PyH_2** is both kinetically and thermodynamically proficient in reducing CO_2 to CH_3OH through three successive homogeneous HTPT steps (Sections 3.4−3.7); and (4) show that the catalytic hydride transfer reaction by the **PyH_2**/Py redox couple is driven by a dearomatization−aromatization process (Section 3.8).[46] Concluding remarks are given in Section 4.

2. COMPUTATIONAL METHODS

We compute stationary geometries (reactants, transition states, and products) for all systems studied using density functional theory based on the M06 density functional[47] and 6-31+G** basis set[48] and a water solvent model described below. The M06 functional was chosen because it has been parametrized with experimental thermodynamic data and should provide a reliable description of the molecular structures for the reactions of interest.[47] To further improve the reported energies, we performed single point energy calculations at the M06/6-31+G** geometries using second order Møller−Plesset perturbation theory (MP2)[49] with the extensive aug-ccPVTZ basis sets.[50] We previously found that MP2 accurately reproduces the CCSD(T) reaction and transition state (TS) energies for reactions between pyridine (Py) and CO_2[46] and have further benchmarked this method against CCSD(T) for reactions involving HT to CO_2, as summarized in Table S1 of the Supporting Information, Section 1.

An adequate treatment of solvent is crucial to correctly describe reactions involving a polar TS, such as those involving electron, proton, or hydride transfers, which are of particular interest here. Therefore, we employed the implicit polarized continuum solvation model (CPCM) in all calculations to treat the solute−solvent electrostatic interactions in aqueous solvent.[51,52] In addition to the CPCM description, in the direct hydride transfer models, DHT-1H_2O and DHT-2H_2O of Section 3.3, we explicitly included one and two water molecules to quantum mechanically model the solvent polarization essential for correctly describing the ionic HT TS. In addition to stabilizing the TS, these water molecules also intimately participate in the reaction by acting as a proton relay chain during the proton transfer event.[46,53−66] The treatment of explicit waters is discussed in greater detail in Supporting Information, Section 1d.

We calculate vibrational force constants at the M06/6-31+G** level of theory to (1) verify that the reactant and product structures have only positive vibrational modes, (2) confirm that each TS has only one imaginary mode and that it connects the desired reactant and product structures via Intrinsic Reaction Coordinate (IRC) calculations, and (3) compute entropies, zero-point energies (ZPE) and thermal corrections included in the reported free energies at 298 K.

For the activation and reaction enthalpies, entropies, and free energies for each of the various reactions examined within, we define the reference state as the separated reactants in solution, as is appropriate for solution-phase bimolecular reactions.[67] It is important to recognize that commonly employed entropy evaluations within the rigid rotor, harmonic oscillator, and ideal gas approximations normally overestimate the entropic cost for reactions occurring in solution phase because ideal gas partition functions do not explicitly take into account hindered translation, rotation, and vibration of the solute surrounded by solvent molecules.[25,68−73] For example, Huang and coworkers observed that the calculated standard activation entropy values ($-T\Delta S^{\ddagger}_{calc}$) consistently overestimate the experimental $-T\Delta S^{\ddagger}_{exp}$ values by ∼4−5 kcal/mol at 298 K.[70,71] Liang and coworkers also observed that $-T\Delta S^{\ddagger}_{exp}$ values are 50−60% of the computed $-T\Delta S^{\ddagger}_{calc}$, and, in some cases, activation entropic costs $-T\Delta S^{\ddagger}_{exp}$ are overestimated by ∼11 kcal/mol.[69] In Supporting Information, Section 2, we show that $-T\Delta S^{\ddagger}_{calc}$ overestimates $-T\Delta S^{\ddagger}_{exp}$ by ∼12 kcal/mol for the analogous HT reaction from the **PyH_2**-related dihydropyridine 1-benzyl-1,4-dihydronicotinamide (in eq 1). Clearly, ideal gas-based calculated $-T\Delta S^{\ddagger}_{calc}$ values can have significant errors.

Although various empirical correction factors for $-T\Delta S^{\ddagger}_{calc}$ values have been proposed,[25,68,73,74] all of which significantly lower $-T\Delta S^{\ddagger}_{calc}$, our approach to better estimate $-T\Delta S^{\ddagger}$ is to employ the experimentally obtained $-T\Delta S^{\ddagger}_{exp}$ value for an analogous HT reaction; as we discuss later, the transition states for all three steps in reduction of CO_2 to CH_3OH are of HT character. This $-T\Delta S^{\ddagger}_{exp}$ value is then added to our calculated $\Delta H^{\ddagger}_{HT}$ in order to obtain more accurate estimates to the activation free energy $\Delta G^{\ddagger}_{HT}$. In particular,

dx.doi.org/10.1021/ja510131a | J. Am. Chem. Soc. XXXX, XXX, XXX−XXX

the homogeneous HT from the **PyH_2**-related dihydropyridine 1-benzyl-1,4-dihydronicotinamide to Δ^1-pyrroline-2-carboxylic acid (zwitterionic form) in aqueous methanol (eq 1)[75] is analogous to each of the three HTs from **PyH_2** of interest here: to CO_2, formic acid (HCOOH), and formaldehyde (OCH_2). We thus add the $-T\Delta S^{\ddagger}_{exp}$ of 2.3 kcal/mol (298 K) determined experimentally for eq 1[75] to the calculated $\Delta H^{\ddagger}_{HT}$ values in Table 1 to obtain our estimates for $\Delta G^{\ddagger}_{HT}$. This procedure is further discussed in Section 3.5. As comparison, we also employed the approach of Morokuma and co-workers[76] to omit the translational contribution from computed gas-phase entropies. We obtained $-T\Delta S^{\ddagger}_{calc}$ = 3.0, 2.2, and 2.7 kcal/mol for the reduction of CO_2, formic acid, and formaldehyde, respectively (via the DHT-1H_2O model defined in Section 3.3); these values are similar to the experimental $-T\Delta S^{\ddagger}_{exp}$ of 2.3 kcal/mol for eq 1 that we have employed. See Supporting Information, Section 2 for details.

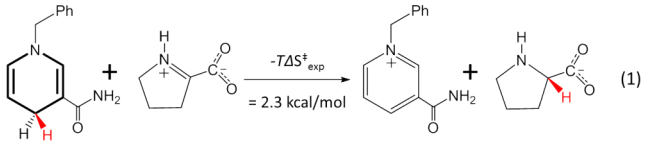

(1)

Finally, reaction free energies (ΔG^0_{rxn}) are reported by adding ΔH^0_{rxn} to $-T\Delta S^0_{rxn}$ in Table 1. Because the number of species remains constant on going from reactants to products in the HTPT reactions described here, the overestimation issue for the calculated $-T\Delta S^0_{rxn}$ is less severe. All reported energies were referenced to separated reactants in solution (as noted above), and calculations were performed using the GAUSSIAN 09[77] and GAMESS[78] computational software packages. Often, reported bimolecular reaction activation and thermodynamic quantities in the literature are referenced to reactants within a reactant complex rather than to the separated reactants. Thermodynamic quantities with the former reference are given for comparison in Supporting Information, Section 3.

3. RESULTS AND DISCUSSION

3.1. Formation of PyH^0 from Py via $1H^+/1e^-$ Transfers.

We begin with the key issue of the generation of PyH^0 from Py via sequential PT-ET steps. In Scheme 2, route **I**, Py first

Scheme 2. Formation of Pyridinium Radical (PyH^0)

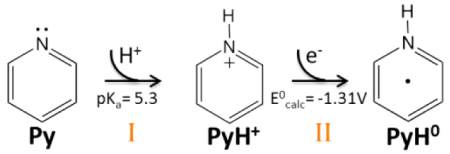

undergoes protonation to form pyridinium (PyH^+; pK_a= 5.3) in a pH 5 solution. Subsequent $1e^-$ reduction (route **II**) produces PyH^0. Experimentally, photoexcited electrons of the p-GaP semiconductor are sufficiently reducing to populate PyH^+'s LUMO ($E^0_{calc} \sim -1.3$ V vs SCE)[46,79,80] via $1e^-$ transfer to form solution-phase PyH^0.[81] For example, at a pH of 5, the conduction band minimum of p-GaP (E_{CBM})[82,83] lies at approximately −1.5 V vs SCE,[84,85] a more negative potential than PyH^+'s LUMO. Furthermore, the p-GaP electrode is electrochemically biased by −0.2 to −0.7 V,[23] which further increases the reducing ability of the transferring electron.

We pause to consider other PyH^0 generation routes. PyH^0 can also be produced electrochemically at inert electrodes. For instance, a glassy carbon electrode[86−88] has been used to electrochemically produce similar neutral radicals from the Py-related species nicotinamide and acridines.[43−45] In another case, photochemical production of PyH^0 driven by visible light was recently demonstrated by MacDonnell and co-workers using a surface-free photochemical process in which Ru(II) trisphenanthroline (chromophore) and ascorbate (reductant) act in concert to reduce PyH^+ to PyH^0 via $1e^-$ transfer.[89−91] The produced PyH^0 radical is actively involved in the observed homogeneous reduction of CO_2 to CH_3OH (albeit at low yield),[89−91] an observation in contrast with recent studies focused on the specific case using a Pt cathode[80,86,92−96] that rule out participation of homogeneous PyH^0 in Py-catalyzed CO_2 reduction. We stress that we consider a Pt electrode to be a special case. There, $1e^-$ reduction of PyH^+ is favored to form adsorbed H atoms (Pt−H*)[94−98] such that its use introduces additional routes (e.g., H_2 formation) that likely outcompete any processes catalyzed by Py. Therefore, surface pathways[93,95] for CO_2 reduction on Pt may predominate such that the homogeneous mechanism discussed in the text requiring the production of PyH^0 becomes a minor pathway. Nonetheless, the mechanism we elucidate involving hydride and proton transfers by dihydropyridines may provide useful insights into any presumably minority surface-mediated pathways that may occur on active cathodes (including Pt).

The conversion of the produced solution-phase PyH^0 to the desired intermediate **PyH_2** will be taken up in Section 3.2. Here, we pause to discuss some competing routes. The first of these arises because PyH^0 is a dearomatized species driven to donate an electron in order to recover its aromaticity.[46,99] For example, Bocarsly and co-workers[33,100] proposed that PyH^0 reacts with CO_2 to form a pyridine-carbamate ($PyCOOH^0$) intermediate (Scheme 3, route **III**) prior to CH_3OH

Scheme 3. $1e^-$ Reduction of CO_2 by PyH^0 To Form $PyCOOH^0$ and Self-Radical Quenching Reactions of PyH^0

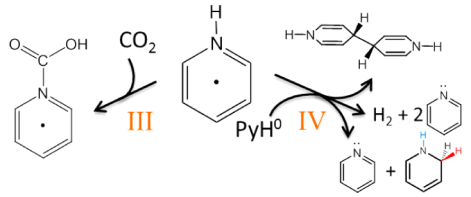

formation.[33] $PyCOOH^0$ formation by this route is supported by our recent computational study[46] and spectroscopic measurements.[101] In particular, using a hybrid explicit/implicit solvent model, we calculated low enthalpic barriers with respect to the complexed reactants of 13.6−18.5 kcal/mol (depending on the number of solvating waters) for $PyCOOH^0$ formation via a proton relay mechanism; the importance of proton relays have been extensively described in assorted chemical reactions.[53−64] Charge analysis on CO_2 and PyH^0 along the reaction coordinate reveals that PyH^0's propensity to recover its aromaticity drives the sequence of ET to CO_2 followed by PT (mediated by a proton relay) to ultimately form $PyCOOH^0$.[46,102] Although this particular reaction is not of direct interest in the present work (see the end of Section 3.2), we will see that the themes of aromaticity recovery and proton relay mechanisms also prove to be important for our three HTPT step reduction of CO_2 to CH_3OH.

Another oxidation channel for PyH^0 is via radical self-quenching, shown in route **IV**. PyH^0 undergoes self-quenching[103] to form either H_2 + 2Py or a 4,4′ coupled dimer;[97,104] the recovery of Py catalyst from the 4,4′ coupled dimer is demonstrated in Supporting Information, Section 4. Interestingly, the PyH^0 self-quenching can also lead to a productive outcome: disproportionation[105] of two PyH^0 radicals leads to Py and the desired **PyH_2** species.[106] However,

dx.doi.org/10.1021/ja510131a | J. Am. Chem. Soc. XXXX, XXX, XXX−XXX

we consider that the main route to **PyH_2** is not this, but instead is via a successive PT and ET to PyH^0,[107,108] now described.

3.2. Formation of 1,2-Dihydropyridine (PyH_2) from PyH^0 via Successive $1H^+/1e^-$ Transfers. We now discuss production of **PyH_2** from PyH^0 via routes **V** and **VI** of Scheme 4 in which PyH^0 undergoes further $1H^+$ and $1e^-$ transfers to

Scheme 4. Formation of 1,2-Dihydropyridine (PyH_2)

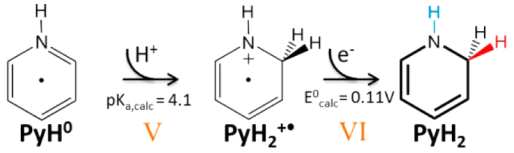

form closed-shell solution-phase **PyH_2**. We propose that these routes are competitive with, if not predominant over, Scheme 3's routes **III** and **IV**. In particular, given that quenching routes (IV) are second-order in $[PyH^0]$ and that routes **III** and **V** are first-order in $[PyH^0]$, it is likely that quenching would prevent the concentration of PyH^0 from reaching a level at which the second-order process dominates. Furthermore, a significant fraction of any self-quenching of PyH^0 that does occur could lead to the desired **PyH_2** species, as observed experimentally for quenching of the related 3,6-diaminoacridinium radical to form the corresponding dihydropyridine species (3,6-diaminoacridan).[105,106]

The protonation of PyH^0 by our proposed route **V** depends on the rate of PT to PyH^0, which we now address in some detail. The pK_a of $PyH_2^{+\bullet}$ is calculated to be 4.1 (at the C_2 carbon),[109−111] indicating that at a pH of 5, ∼13% of PyH^0 is protonated in the bulk solution. However, in the case of photoelectrochemical reduction on a p-GaP cathode, PyH^0 is produced by reduction of PyH^+ at the cathode near the double layer region, where the lower pH facilitates its protonation to form $PyH_2^{+\bullet}$. The key here is that near the double layer region the electric field created by the applied negative bias at the cathode concentrates cationic PyH^+ and H_3O^+ species according to a Poisson−Boltzmann distribution,[112−114] lowering the pH near the cathode surface. For example, in Supporting Information, Section 5, we use a linearized Poisson−Boltzmann model to show that the concentrations of cation acids, e.g., H_3O^+ and PyH^+, increase considerably as they approach the negatively biased cathode. Although these calculations are certainly not quantitative very near the cathode, our estimate at ∼5 Å of a factor of ∼10 increase in $[H_3O^+]$ and $[PyH^+]$ from their bulk values is reasonable. A decrease of the effective pH by one unit to a pH of 4 raises the percentage of PyH^0 protonated by PyH^+ or H_3O^+ from ∼13 to ∼50%. Thus, protonation of PyH^0 by PyH^+ or H_3O^+ near the cathode double layer to form the desired radical cation $PyH_2^{+\bullet}$ becomes a quite probable event with a much higher probability than radical self-quenching via route **IV** because $[\text{cation acids}] \gg [PyH^0]$.

It is noteworthy that the lack of any negative cathode double layer assistance in the surface-free Ru(II)/ascorbate photochemical system mentioned in Section 3.1 is consistent with the observation that high PyH^+/Ru(II) ratios of ∼100 were required to produce CH_3OH, which we suggest is required to drive protonation of PyH^0 in a cathode's absence.[89]

Finally, **PyH_2** is produced by reduction of $PyH_2^{+\bullet}$ in proposed route **VI** in Scheme 4; our calculated positive reduction potential for $PyH_2^{+\bullet}$ of E^0_{calc} = 0.11 V vs SCE indicates that $PyH_2^{+\bullet}$ reduction is facile and consequently that $1e^-$ transfer (from PyH^0 or via a photoexcited electron) to $PyH_2^{+\bullet}$ to form **PyH_2** is realized on p-GaP and in the homogeneous Ru(II)/ascorbate photochemical system. We note that in the presence of an electrode (e.g., p-GaP), $1e^-$ reduction of $PyH_2^{+\bullet}$ occurs near the double layer to form **PyH_2**, although diffusion of the neutral **PyH_2** into the reaction layer and bulk solution allows catalytic homogeneous HT reaction to occur.

Our suggested sequential PT−ET−PT−ET sequence (Schemes 2 and 4, routes **I**, **II**, **V**, and **VI**) to form **PyH_2** from Py is strongly supported by the fact that an analogous process has been observed for the conversion of the Py-related species nicotinamide,[43,115] acridine,[44,116] and 3,6-diaminoacridine (proflavine)[45] to their related dihydropyridine species. We point out that we propose the formation of 1,2-dihydropyridine as the kinetic product[39] because protonation of the PyH^0's C_2 carbon is more facile than protonation at the C_4 position,[109] analogous to protonation of nicotinamide where the related 1,2-dihydropyridine is formed.[43] However, 1,4-dihydropyridine can also be produced, although at a slower rate.[39] In Supporting Information, Section 6, we show both dihydropyridine species

Scheme 5. Reductions via Direct Hydride Transfers from Related Dihydropyridine Species[a]

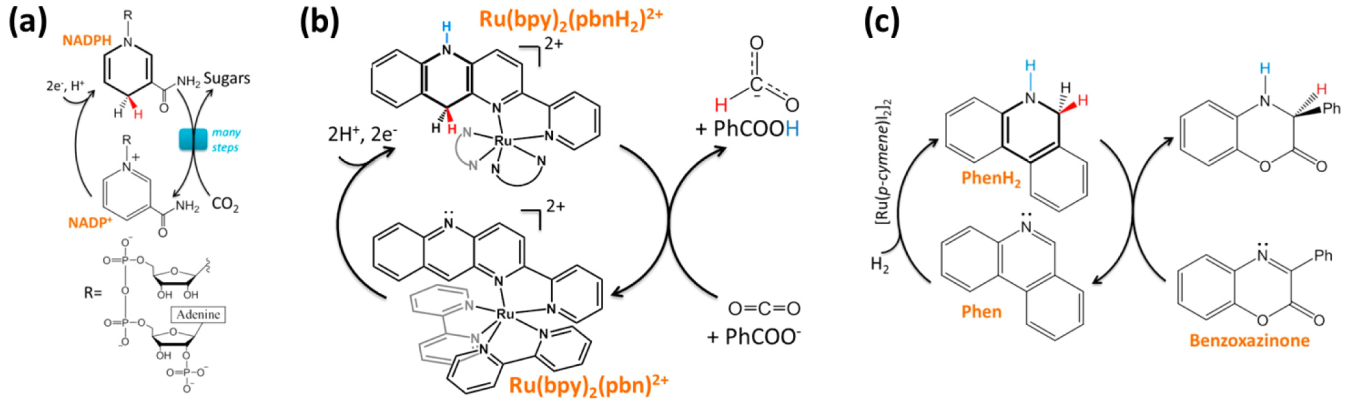

[a](a) NADPH/$NADP^+$ redox cycle of photosynthesis to produce sugars from CO_2 by hydride transfers. NADPH creates a C−H bond by HT to a carbonyl group, not in CO_2, in a key reduction in the multistep photosynthetic process. (b) Catalytic reduction of CO_2 to formate via HT involving Tanaka's Ru-based dihydropyridine species (**$Ru(bpy)_2(pbnH_2)^{2+}$**); bpy = 2,2′-bipyridine, pbn = 2-(pyridin-2-yl)benzo[b][1,5]naphthyridine).[29,121] (c) Catalytic hydrogenation (via hydride and proton transfer) of benzoxazinone by Zhou's dihydrophenanthridine species (**$PhenH_2$**).[122]

dx.doi.org/10.1021/ja510131a | J. Am. Chem. Soc. XXXX, XXX, XXX−XXX

to be capable of direct HT, with 1,2-dihydropyridine being the slightly more reactive species. We also note that acid-catalyzed hydration of both 1,2-dihydropyridine and 1,4-dihydropyridine may generate undesirable side products.[117,118]

The focus of this work is to demonstrate the formation of **PyH$_2$** and its subsequent hydride transfer reactions to form methanol (Scheme 1). Routes **III** (PyCOOH^0 formation), **IV** (radical quenching), and **V** (PT to PyH^0) are all bimolecular reactions with corresponding rate constants of ~10^0,[46] ~10^9,[103] and ~10^4–10^9 M^{-1} s^{-1},[107] respectively. Under the commonly employed experimental conditions/concentrations, the rates of routes **IV** and **V** are both expected to be concentration-dependent, whereas the rate of route **III** is activation-dependent. Therefore, we expect the contribution of route **III** to be minor under these conditions, but we note that insufficient evidence exists to conclude the fate of PyCOOH^0 species; thus far, there is also no experimental verification for the existence of PyCOOH^0 species (as well as several intermediates leading to methanol production) produced under electrochemical/photoelectrochemical conditions.

We have thus far described likely steps that transform Py into **PyH$_2$**, a species that we now show to be competent in performing catalytic direct HT to carbonyls.

3.3. Establishing the Hydride Nucleophilicity of PyH$_2$ and Related Dihydropyridines. First, it is noteworthy that **PyH$_2$** chemically resembles the NADPH dihydropyridine species found in nature (Scheme 5a and caption) that acts in the NADPH/NADP$^+$ redox cycle of photosynthesis to produce sugars from CO_2 by hydride transfers.[119,120] In particular, NADPH creates a C–H bond by HT to a carbonyl group, not in CO_2, in a key reduction in the multistep photosynthetic process. Although HT from NADPH is catalyzed by enzymes, both NADPH and **PyH$_2$** share the same dihydropyridine core, the 2e$^-$/1H$^+$ redox cycle that produces the dihydropyridines and the subsequent HT chemistry. More generally, since the discovery of NADPH in the 1930s, related dihydropyridine compounds have been studied, especially in connection with their HT to various substrates containing C=C, C=N, and C=O groups.[39–42] HT to carbonyls is obviously of particular interest here: the reactant CO_2 and its reduced intermediates formic acid (HCOOH) and formaldehyde (OCH_2) leading to CH_3OH formation all contain C=O groups susceptible to HT.

Here, we mention two examples of related recyclable dihydropyridines performing HT to the C=O and C=N groups. Tanaka and co-workers demonstrated[121] (Scheme 5b) that the electrochemical reduction of Ru(bpy)$_2$(pbn)$^{2+}$ forms the NADPH-like **Ru(bpy)$_2$(pbnH$_2$)$^{2+}$**, where the pbn ligand has undergone 2H$^+$/2e$^-$ transfer to form a dihydropyridine-like hydride donor.[123] Association of **Ru(bpy)$_2$(pbnH$_2$)$^{2+}$** with a benzoate base (PhCOO$^-$) then activates its hydride donation to CO_2 to form HCOO$^-$ and PhCOOH and to concomitantly regenerate Ru(bpy)$_2$(pbn)$^{2+}$.[29] An H/D kinetic isotope effect of 4.5 further supports the direct hydride transfer mechanism to CO_2 to form HCOO$^-$.[29] Similarly, Zhou et al.'s dihydrophenanthridine (**PhenH$_2$**), a **PyH$_2$** analogue, catalytically transfers both its hydride and proton to benzoxazinone and regenerates the phenanthridine catalyst (Scheme 5c), further demonstrating the competence of dihydropyridine species as recyclable hydride donors.[122]

We have thus far argued that the HT reactivity of related dihydropyridine hydrides **NADPH**, **Ru(bpy)$_2$(pbnH$_2$)$^{2+}$** and **PhenH$_2$**, especially the extraordinary ability of **Ru(bpy)$_2$(pbnH$_2$)$^{2+}$** to effect CO_2 reduction, strongly implicates **PyH$_2$** as a robust hydride donor in Py-catalyzed CO_2 reduction. The next step is to quantify **PyH$_2$**'s ability as a hydride donor, i.e., its hydride nucleophilicity. Figure 1 shows the quantification of this aspect of hydride donors using Mayr and co-workers' nucleophilicity (N) values,[124,125] where large N values indicate strong hydride donor ability. Note that the N scale is a kinetic parameter quantifying the HT rate, whereas the often-employed hydricity is a thermodynamic parameter.[126–128] In order to place the N values of **PyH$_2$** and Zhou's **PhenH$_2$** in perspective relative to established values for dihydropyridines and $NaBH_4$, we calculate activation free energies for HT ($\Delta G^{\ddagger}_{HT}$) from these donors to CO_2 to reduce it to formate ($HCOO^-$) via the direct hydride transfer (DHT) model illustrated in Figure 2a.

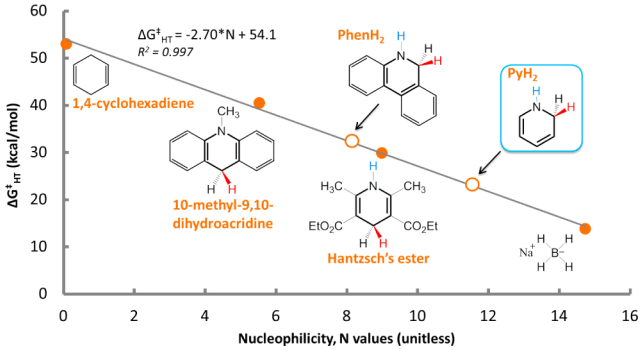

Figure 1. Activation free energy of hydride transfer to CO_2 varies linearly with hydride nucleophilicity. $\Delta G^{\ddagger}_{HT}$ (kcal/mol) is our calculated activation free energy for direct HT to CO_2 to form $HCOO^-$. $\Delta G^{\ddagger}_{HT}$ is obtained by adding our calculated $\Delta H^{\ddagger}_{HT}$ to the experimental $-T\Delta S^{\ddagger}_{exp}$ = 2.3 kcal/mol for the analogous HT reaction eq 1, with all quantities referenced to the separated reactants (see Section 2). Nucleophilicity (N) values quantify the strength of hydride donors.[124,125] The equation log k(20 °C) = $s(N + E)$ was used to obtain N and s (the slope factor) values in order to generalize various classes of hydride donors, including dihydropyridines and borohydrides. HT rate constants k are measured at 20 °C for HT to acceptors with known E (electrophilicity) values. Our calculated $\Delta G^{\ddagger}_{HT}$ values are used to estimate k and thus N values of **PyH$_2$** and Zhou's **PhenH$_2$** relative to established N values for dihydropyridines and $NaBH_4$. These $\Delta G^{\ddagger}_{HT}$ values are obtained with CO_2 acting as the hydride acceptor; CO_2's E value is unknown, but this is immaterial to the estimation of **PyH$_2$** and **PhenH$_2$**'s N values.[129] The comparatively low $\Delta G^{\ddagger}_{HT}$ and high hydride nucleophilicity of **PyH$_2$** are apparent in this figure.

In Figure 1, we use the experimental N and our calculated $\Delta G^{\ddagger}_{HT}$ values (in kcal/mol) of 1,4-cyclohexadiene (0.09, 53.0),

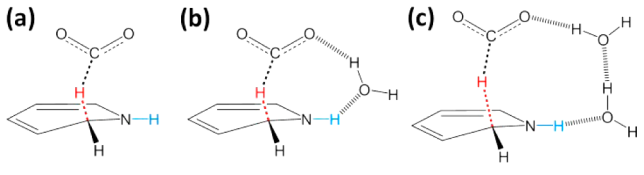

Figure 2. HT to CO_2 can occur through various direct HT configurations. Here, we model three possible HT configurations, without (a) and with (b, c) the active participation of H_2O, which we demonstrate are kinetically and thermodynamically favorable toward reducing CO_2: (a) direct hydride transfer (DHT) model, (b) DHT-1H_2O model where one H_2O acts as a proton relay, and (c) DHT-2H_2O model where two H_2O's act as a proton relay. Details of these relays are discussed subsequently.

dx.doi.org/10.1021/ja510131a | J. Am. Chem. Soc. XXXX, XXX, XXX–XXX

10-methyl-9,10-dihydroacridine (5.54, 40.5), Hantzsch's ester (9.00, 29.9), and $NaBH_4$ (14.74, 13.8) to obtain a nearly linear relationship between $\Delta G^{\ddagger}_{HT}$ and N: $\Delta G^{\ddagger}_{HT} = -2.70N + 54.1$.[130] We then use this linear relation together with our calculated $\Delta G^{\ddagger}_{HT}$ barriers to estimate that the N values of **PhenH$_2$** and **PyH$_2$** are 8.1 and 11.4, respectively. Although **PyH$_2$** is a less capable hydride donor than the well-known strong donor $NaBH_4$, it is the most reactive dihydropyridine, reducing CO_2 to $HCOO^-$ at $\Delta G^{\ddagger}_{HT}$ = 23.2 kcal/mol by the DHT model. The hydricity of **PyH$_2$** was also calculated according to Muckerman et al.'s approach;[128] we obtained 41.5 kcal/mol (<43 kcal/mol of $HCOO^-$), which supports that HT from **PyH$_2$** to CO_2 is thermodynamically favorable.[131] We note that although cyclic voltammetry shows that the oxidation of **PyH$_2$**-related dihydronicotinamide by ET−PT−ET−PT is irreversible and indicates that it is a poor electron transfer catalyst,[115] this does not preclude dihydronicotinamide or dihydropyridines in general from being competent hydride transfer catalysts.

With these important preliminaries concerning **PyH$_2$**'s generation and HT ability concluded, we now turn to the three HTPT steps in the reduction of CO_2 to methanol.

3.4. First HTPT Step: PyH$_2$ + CO$_2$ → Py + HCOOH. We now elaborate the first HTPT step in CO_2's conversion to CH_3OH: HT to CO_2 by **PyH$_2$** to form formic acid (HCOOH). This step is illustrated in Scheme 6, route **VII**, although, as we will see, there are two sequential steps involved, namely, first formate ion $HCOO^-$ production followed by formic acid generation.[132] $\Delta G^{\ddagger}_{HT}$ for this step without the electrostatic effects and active participation of the proton relay (predicted using the DHT model in Figure 2a) is 23.2 kcal/mol. This shows that even without the effects described by explicit water, HT is kinetically viable.

Scheme 6. Reduction of CO$_2$ to Formic Acid by PyH$_2$

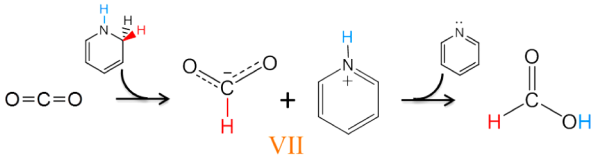

In an attempt to improve the description beyond the DHT model, we have considered two likely elaborations in aqueous solution. We added one and two solvating water molecules (DHT-1H_2O and DHT-2H_2O, Figure 2b,c) to polarize the reactive complex beyond the polarization afforded by implicit solvent and thus stabilize the ionic TS relative to the neutral reactants. As will be seen, in the formic acid and formaldehyde reductions, the solvating water molecule(s) play an additional, more active role; they act as a proton relay, for which this mixed explicit/implicit solvation approach[58,59,133] is especially important for an accurate description.[46,53−56] For the DHT-1H_2O and DHT-2H_2O models, we obtain barriers of $\Delta G^{\ddagger}_{HT}$ = 17.1 and 14.3 kcal/mol for the CO_2 reduction to $HCOO^-$, ∼6 and 9 kcal/mol lower than for the DHT model, reflecting the importance of quantum mechanically described water polarization (Table 1).

Analysis of the reaction path using an IRC calculation shows that the TS is of HT character such that the use of the experimental HT activation entropy discussed at the end of Section 2 is appropriate.[134] The IRC analysis also shows that the product complex consists of the formate anion $HCOO^-$ and PyH^+; the reaction is pure HT without any PT, even with a proton relay chain of one or more explicit water molecules included. Because HCOOH's pK_a of 3.8 is relatively low, the carbonyl of $HCOO^-$ is not basic enough to abstract a proton from its neighboring H-bonded water to initiate a proton relay that would effectively transfer the proton from PyH^+ to $HCOO^-$. In contrast, in Sections 3.5 and 3.6, we will show that the HT intermediary products of formic acid (hydroxymethanolate $(HCOOH)H^-$) and formaldehyde (methoxide, OCH_3^-) are highly basic and do initiate a proton relay; PyH^+'s proton is effectively transferred to these species through the proton relay to form methanediol and methanol, respectively.

Thus, with all three models, the formate product remains unprotonated. However, for the next HTPT step to proceed, $HCOO^-$ must first be protonated to form formic acid (HCOOH). HCOOH's pK_a of 3.8 indicates that at equilibrium, 298 K and pH 5, only $\sim^1/_{16}$ of $HCOO^-$ is protonated to produce HCOOH; such a low [HCOOH] combined with its high reduction barrier (*vide infra*) leads to the observed formate accumulation in the homogeneous Ru(II)/ascorbate photochemical system.[89] However, heterogeneous assistance (not shown explicitly in Scheme 6) can be provided by a cathode, as described in Section 3.2; the enhanced concentrations of H_3O^+ and PyH^+ near the cathode (e.g., p-GaP)[33,112] increases the concentration of HCOOH in equilibrium with $HCOO^-$ which increases the reduction rate in the reaction layer.

Table 1. Activation and Reaction Free Energies and Enthalpies for HTPT Steps from PyH$_2$ to CO$_2$, HCOOH, and OCH$_2$ via Various HT Models in Figure 2

	CO_2[b]		HCOOH[c]		OCH_2[d]	
model[a]	$\Delta G^{\ddagger}_{HT}$ ($\Delta H^{\ddagger}_{HT}$)	ΔG^{0}_{rxn} (ΔH^{0}_{rxn})	$\Delta G^{\ddagger}_{HT}$ ($\Delta H^{\ddagger}_{HT}$)	ΔG^{0}_{rxn} (ΔH^{0}_{rxn})	$\Delta G^{\ddagger}_{HT}$ ($\Delta H^{\ddagger}_{HT}$)	ΔG^{0}_{rxn} (ΔH^{0}_{rxn})
DHT	23.2 (20.9)	−9.2 (−5.5)	25.6 (23.3)	−12.8 (−12.8)	14.5 (12.2)	−31.3 (−31.4)
DHT-1H_2O	17.1 (14.8)	−8.3 (−10.8)	23.4 (21.1)	−10.6 (−10.8)	8.9 (6.6)	−31.9 (−31.8)
DHT-2H_2O	14.3 (12.0)	−5.6 (−9.8)	18.7 (16.4)	−11.9 (−12.2)	6.0 (3.7)	−30.8 (−31.9)

[a]All free energies and enthalpies, referenced to separated reactants in solution, are reported in kcal/mol at 298 K and 1 atm. [b]$2e^-/2H^+$ transfer product, formic acid. [c]$2e^-/2H^+$ transfer product, methanediol. [d]$2e^-/2H^+$ transfer product, methanol. The CO_2 pathway involves a sequential HT (to produce formate) followed by cathode-assisted PT (to produce formic acid); the activation barriers displayed refer to the HT portion of the reaction. The formic acid and formaldehyde reduction pathways both involve a coupled HTPT process, where **PyH$_2$** transfers both its hydridic and protic hydrogens to HCOOH and OCH_2, respectively: each case involves a single TS of HT character, with the PT following at a slightly later time, without a separate TS. The formaldehyde reduction step is preceded by the dehydration of methanediol to formaldehyde ($K_{eq} \sim 5 \times 10^{-4}$); see Figure 3 and Section 3.6. Calculated imaginary frequencies corresponding to the transition state structures are reported in the Supporting Information, Section 8.

dx.doi.org/10.1021/ja510131a | J. Am. Chem. Soc. XXXX, XXX, XXX−XXX

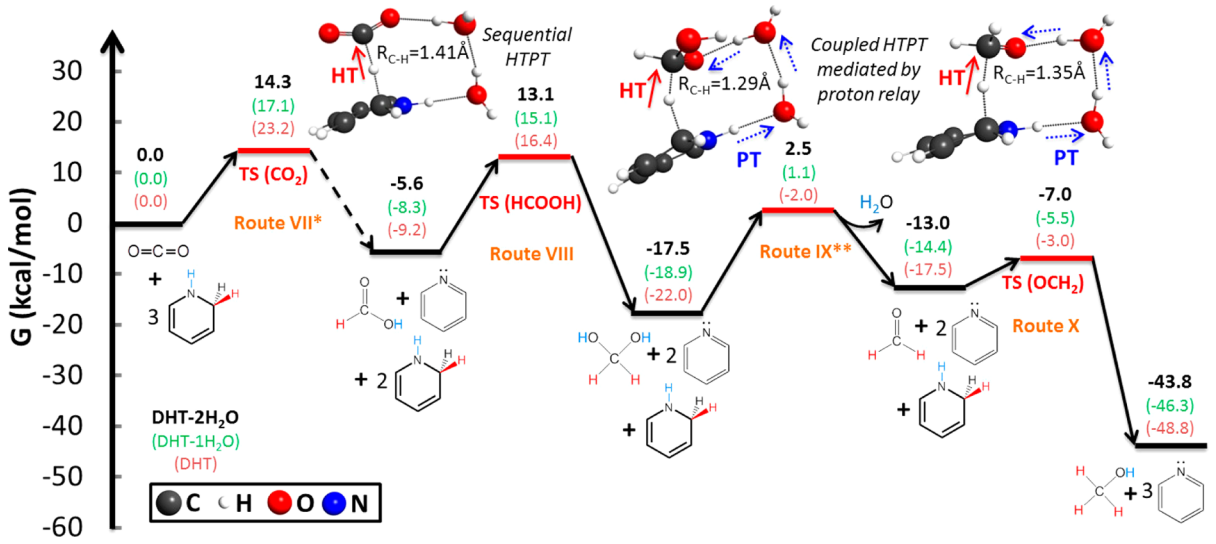

Figure 3. Conversion of CO_2 to CH_3OH and H_2O by **PyH_2** proceeds through three hydride and proton transfer steps. The reported free energies correspond to stationary points along the reaction potential energy surface using the DHT-2H_2O (black), DHT-1H_2O (green), and DHT (orange) models, catalyzed by HTPT reactions of the **PyH_2**/Py redox couple. The first HTPT step (Scheme 6, route **VII**) is sequential, where HT from **PyH_2** to CO_2 forms stable formate ($HCOO^-$), with a single TS of HT character, and subsequent PT follows to produce formic acid (HCOOH) (*the dashed line indicates that the product of HT to CO_2 is formate where a separate cathode-enhanced protonation step forms formic acid.) In the second HTPT step (Scheme 7, route **VIII**), homogeneous coupled HTPT occurs with a single TS: HT from **PyH_2** to HCOOH, which dominates the barrier and is followed by PT without an additional TS (from oxidized **PyH_2**, essentially a PyH^+), is mediated by a proton relay involving water molecules, ultimately producing methanediol ($CH_2(OH)_2$). Prior to the next reduction step, $CH_2(OH)_2$ is dehydrated to form the reactive formaldehyde (OCH_2) species at $K_{eq} \sim 5 \times 10^{-4}$ (Scheme 8, route **IX**); thus, this constitutes an additional free energy activation cost of ~4.5 kcal/mol for OCH_2 reduction. (**The rate constant for the dehydration of $CH_2(OH)_2$ to OCH_2 at 298 K and pH of 6–7.8 is $\sim 5 \times 10^{-3}$ s^{-1} or equivalently the estimated $\Delta G^{\ddagger}_{dehyd}$ is ~20 kcal/mol.[138,139] Consequently, the effective rate constant for transformation of $CH_2(OH)_2$ to CH_3OH is that of $CH_2(OH)_2$ dehydration.) In the third and final, homogeneous, HTPT step (Scheme 8, route **X**), which is similar to HCOOH reduction, coupled HTPT occurs, where HT from **PyH_2** to OCH_2 involves a single TS of HT character and is followed by a proton relay-mediated PT without an additional TS to ultimately form methanol (CH_3OH). During each reaction step, the Py catalyst is recovered, thus confirming that **PyH_2** is a recyclable organo-hydride. TS structures for the HTPT steps from **PyH_2** to CO_2, HCOOH, and OCH_2 are shown for the DHT-2H_2O model. (Coordinates for the TS structures for all three DHT models are reported in Supporting Information, Section 8.) All TS structures are HT in character. Animations of the HTPT steps for the reduction of CO_2, HCOOH, and OCH_2 are available in the Supporting Information.

Thus, the first HTPT step to reduce CO_2 is sequential, with HT (to produce a relatively stable $HCOO^-$ intermediate corresponding to a minimum on the HT potential energy surface) followed by a subsequent cathode-assisted PT (to produce HCOOH), which we write collectively as **PyH_2** + CO_2 → Py + HCOOH. We could also term this stepwise HTPT as *uncoupled* HTPT.

Py and HCOOH formation by **PyH_2** + CO_2 → Py + HCOOH with all three DHT models have negative reaction free energies ΔG^0_{rxn} of ~−9 to −6 kcal/mol, as shown in Table 1. This demonstrates that **PyH_2** is both kinetically and thermodynamically competent in catalytically reducing CO_2, at least for the first HTPT step. We will show that this catalytic ability also holds for the remaining two HTPT steps to attain methanol. The schematic free energy surface for this first HTPT step to transform CO_2 into HCOOH is shown in Figure 3, which also illustrates the free energies of the two subsequent HTPT steps described in Sections 3.5 and 3.6.

We close the discussion of this first CO_2 reduction step with two remarks. First, although we have considered only three models (Figure 2a–c) for HT from **PyH_2** to CO_2, other configurations, such as DHT-K^+ and DHT-PyH^+ where a potassium cation (present as an electrolyte) and the pyridinium cation act as a Lewis acid and a Brønsted acid, respectively, to activate and stabilize HT[135] to CO_2, can also lead to the desired HCOOH and Py products. Furthermore, because the reaction is carried out in aqueous solvent, we propose that DHT-1H_2O, DHT-2H_2O, and other likely DHT models with somewhat longer water proton relay chains contribute significantly to the ensemble-weighted average $\Delta G^{\ddagger}_{HT}$. Second, all reported $\Delta G^{\ddagger}_{HT}$ values in Table 1 (including $\Delta G^{\ddagger}_{HT}$ for the first HTPT step to form HCOOH and Py) are derived by adding our calculated $\Delta H^{\ddagger}_{HT}$ to the experimentally obtained $-T\Delta S^{\ddagger}_{exp}$ = 2.3 kcal/mol for an analogous HT reaction eq 1 (again, all quantities are referenced to separated reactants). This is a significantly more reliable estimate for solution-phase HT from **PyH_2** than a calculated $-T\Delta S^{\ddagger}_{calc}$ based on ideal gas assumptions, which can severely overestimate the entropic contribution to $\Delta G^{\ddagger}$;[25,68–73] see Section 2.

3.5. Second HTPT Step: PyH_2 + HCOOH → Py + $CH_2(OH)_2$. We now turn to the second HTPT step: the homogeneous reduction of formic acid to methanediol ($CH_2(OH)_2$), as illustrated in Scheme 7, route **VIII**. HCOOH's reduction is actually more challenging than that of CO_2, a feature implied by the fact that most CO_2 reduction catalysts

Scheme 7. Reduction of Formic Acid to Methanediol by PyH_2

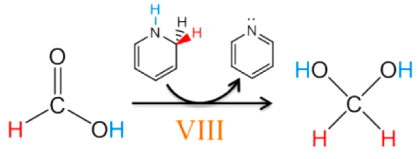

dx.doi.org/10.1021/ja510131a | J. Am. Chem. Soc. XXXX, XXX, XXX–XXX

produce $HCOO^-$/HCOOH but fail to convert HCOOH to more reduced products.[11,14,18] A further indication is provided by the observations of MacDonnell and co-workers, who found a significant buildup of $HCOO^-$ in their photochemical CO_2 reduction study referred to earlier, reflecting the challenge of HCOOH reduction.[89] The key characteristic of HCOOH that makes it difficult to reduce is its highly negative electron affinity (EA); we calculated the gas-phase adiabatic EA of HCOOH to be −1.22 eV, which is significantly more negative than the −0.60 eV EA of CO_2 (see Supporting Information, Section 1c) and indicates that, as noted above, formic acid is even more challenging to reduce than CO_2.[136,137] We now examine **PyH_2**'s ability to reduce HCOOH.

Table 1 summarizes both $\Delta G^{\ddagger}_{HT}$ and ΔG^{0}_{rxn} for the second HTPT step: **PyH_2** + HCOOH → Py + $CH_2(OH)_2$ via the three HT models shown in Figure 2a−c; note that the CO_2 4e$^-$ reduction product methanediol is formed along with the recovery of the Py catalyst. The $\Delta G^{\ddagger}_{HT}$ of 23.4 kcal/mol for the DHT-1H_2O case is ∼2 kcal/mol lower than the DHT barrier (25.6 kcal/mol), whereas the DHT-2H_2O model reaction results in a further lowering of $\Delta G^{\ddagger}_{HT}$ to 18.7 kcal/mol (Figure 3 for the computed TSs for the DHT-2H_2O model). As we will soon see, this reduction only involves a single TS and is thus a *coupled* HTPT process. The character of the TS is primarily that of HT, with PT occurring subsequently without its own TS (as implied in Figure 4, to be discussed). This supports our use of the HT activation entropy factor of Section 2. In fact, because the PT occurs along the exit channel ∼12 kcal/mol below the TS, even an unusually large $-T\Delta S^{\ddagger}$ for PT would not limit the rate of HTPT.

The DHT model results with one and two explicit waters show that HCOOH reduction to generate $CH_2(OH)_2$ is aided by a proton relay chain involving explicit water. Such chains of course stabilize the ionic TS, but they also facilitate PT by reducing strain in the TS, and, in addition, the PT from the H_2O H-bonded to HCOOH (Figure 4) stabilizes the partially reduced product as negative charge accumulates on HCOOH. Consequently, the coupled PT helps to overcome the reduction challenges associated with HCOOH's low EA.

This PT and subsequent PTs in the relay chain occur after the HT barrier (Figure 4a) and of course before the stable products are formed (Figure 4 for the DHT-1H_2O case). Only a very modest activation entropy effect is anticipated here because in the coupled HTPT process the PT step(s) is (are) considerably delayed relative to the HT such that any entropic penalties due to PT contribute to the free energies of structures well past the TS. This view is also supported by the prior configuration of the water molecules in the aqueous solution solvating the reactant complex and the widespread occurrence of proton relays in other processes,[54−56,58,59,63−66] including water oxidation[53,57] and enzymatic reactions.[60−62] In any event, the $\Delta G^{\ddagger}_{HT}$'s reported in Table 1 show that the homogeneous reaction is viable even without involvement of any proton relay chain.

To better understand how coupled HT and PT enables **PyH_2** to reduce formic acid and indeed to further support our statements above concerning its coupled character, we analyze HCOOH's reduction by **PyH_2** and its proton relay process in greater detail. In Figure 4a, we show how DHT-1H_2O's energy (the internal energy E_{0k} calculated at 0 K and not ZPE-corrected) changes from the reactant complex (R) through the TS and structures (i, ii, and iii) energetically downhill from the TS before ultimately reaching the product complex (P) along

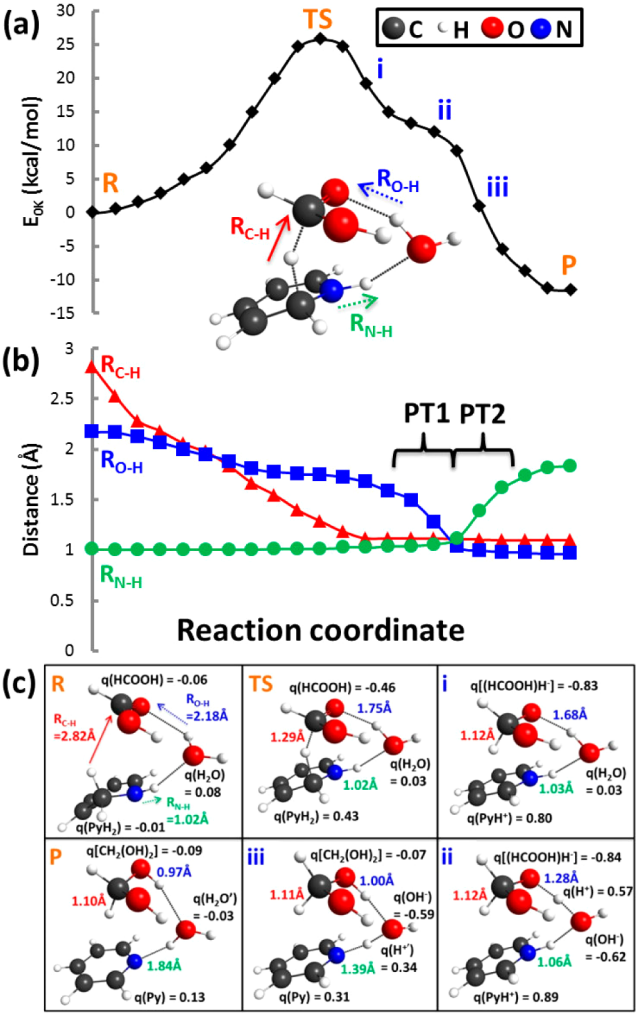

Figure 4. Analysis of the coupled homogeneous HTPT process between **PyH_2** and HCOOH to form Py and $CH_2(OH)_2$ via the DHT-1H_2O model. Similar results are found for HTPT to formaldehyde. Panels: (a) energy (E_{0K}, not ZPE-corrected); R denotes the reactant complex, TS the transition state, i, ii, and iii are structures in the exit channel, and P, the product complex, (b) bond length, and (c) structures and charges q (calculated with the CHELPG method[140] and in the units of e) of important moieties along the reaction coordinate (corresponding to structures in panel a). Both bond length and charge analyses show that the TS is dominated by HT (which is similar to the case of CO_2 reduction by **PyH_2**). Thus, the experimentally obtained $-T\Delta S^{\ddagger}_{exp}$ = 2.3 kcal/mol for a related HT reaction (eq 1) is a good estimate for the $-T\Delta S^{\ddagger}_{HT}$ of the HCOOH reduction, despite the involvement of PT because PT occurs well after the HT TS, although well before the product is formed. Here, PT occurs via proton relay ∼12 kcal/mol below (after) HCOOH's TS. This feature, as well as the absence of a TS for the PT, confirms the coupled character of the HTPT reaction. Because the HT and PT reactions occur in a process characterized by a single free energy TS,[141−145] we have characterized this HTPT process as *coupled*.[146] It is so distinguished from the *uncoupled* HTPT reduction of CO_2 to ultimately produce HCOOH, where the first HT involving a single TS produces the $HCOO^-$ intermediate and subsequently PT to $HCOO^-$ occurs independently to produce HCOOH.

the computed reaction coordinate. Along the same coordinate reaction, we plot the change of key bond lengths (Figure 4b). This analysis shows that the transformation from the reactant to the TS is dominated by HT. That is, R_{C-H} (defined in Figure 4a) shortens from 2.82 Å at R to 1.29 Å at the TS, whereas

dx.doi.org/10.1021/ja510131a | J. Am. Chem. Soc. XXXX, XXX, XXX−XXX

R_{O-H} and R_{N-H} do not change appreciably. Consequently, PT either to HCOOH or from oxidized **PyH_2** does not occur until well past the TS. There is no TS associated with either of these PTs, although PT does produce a shoulder in the potential energy surface ∼12 kcal/mol below the TS caused by HT.

Despite the important distinction between the first two HTPT reduction steps just emphasized, the character of HCOOH's reduction by **PyH_2** is similar to that of the reduction of CO_2 in the sense that HT dominates the energetics leading to the TS for both reactions; thus, as commented in the caption of Figure 4, the experimental $-T\Delta S^{\ddagger}_{exp}$ value of 2.3 kcal/mol for HT from the related dihydropyridine HT reaction (eq 1) is also a reasonable $-T\Delta S^{\ddagger}_{HT}$ estimate for HT to HCOOH by **PyH_2**.

On the other hand, the HCOOH reduction is different from that of CO_2 in that, as we noted above, HCOOH's HT reaction is followed by coupled PT along the reaction coordinate, mediated by a proton relay via H-bonded water molecule(s). The first PT occurs along the exit channel ∼12 kcal/mol downhill from the TS (Figure 4a,b), where the C═O oxygen of the hydroxymethanolate anion ($(HCOOH)H^-$ product of HT to HCOOH) abstracts a H^+ from its H-bonded H_2O to form methanediol and a hydroxide (OH^-)-like moiety (characterized further below). In contrast to CO_2 reduction, where the produced $HCOO^-$ is not basic enough to initiate a proton relay, the HT intermediary product of formic acid, $(HCOOH)H^-$, is sufficiently basic (pK_a of methanediol is ∼13)[147,148] to commence a proton relay by abstracting a H^+ from the neighboring H-bonded water.

This first PT event (PT1) is marked by the shortening of R_{O-H} from ∼1.6 to ∼1.0 Å. Immediately following PT1, the second PT event (PT2) occurs where the just-formed OH^--like moiety now abstracts a H^+ from its H-bonded partner PyH^+ (formed by HT from **PyH_2**) to form H_2O and, more importantly, to recover the Py catalyst. This aspect of the proton relay process is marked by the lengthening of R_{N-H} from ∼1.0 to ∼1.8 Å. This analysis clearly shows the cooperative nature of the HT and PT and that, although the PTs occur well into the exit channel, they act to stabilize the HT TS without participating in the TS's configuration.

Finally, we analyze how the charges on various moieties change along the reaction coordinate. In Figure 4c, it is apparent that as the reaction proceeds from R to TS the charge of **PyH_2** becomes increasingly positive (q = 0.43e), whereas HCOOH becomes increasingly negative (q = −0.46e); this is consistent with a HT reaction and correlates with the motions along the reaction coordinate in Figure 4b. As the hydride transfer from **PyH_2** to the HCOOH carbon becomes more complete (structure i), the $(HCOOH)H^-$ moiety becomes increasingly basic (q = −0.83e) such that its carbonyl oxygen begins to abstract a proton from the H-bonded water molecule (structure ii) to form an intermediate hydroxide OH^- type moiety (q = −0.62e). Structure iii shows that this basic species then abstracts a proton from PyH^+, completing the proton relay to ultimately produce $CH_2(OH)_2$ while recovering the Py catalyst in the product P; H_2O' denotes a newly formed water as a result of proton relay. Figure 4 shows that **PyH_2** contains both hydridic (C_2−H) and protic (N−H) hydrogens; this is analogous to the situation for ammonia borane, which we previously showed reduces CO_2 by HTPT.[37,38]

3.6. Third HTPT Step: $PyH_2 + OCH_2 \rightarrow Py + CH_3OH$. We now address the third and final reduction step to produce the desired product, CH_3OH. This homogeneous step follows the formation of $CH_2(OH)_2$, which is a hydrated formaldehyde (OCH_2). To effect further reduction, the sp^3-hybridized $CH_2(OH)_2$ produced by the second HTPT must first be dehydrated to form the sp^2-hybridized species OCH_2 at $K_{eq} \sim 5 \times 10^{-4}$ (Scheme 8, route **IX**).[149] Although equilibrium strongly

Scheme 8. Dehydration of Methanediol To Form Formaldehyde and the Subsequent Reduction to Methanol by PyH_2

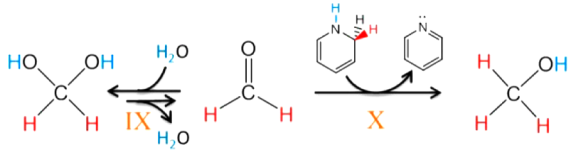

favors the diol species, OCH_2 is significantly more reactive to HT, producing methanol via **PyH_2** + $OCH_2 \rightarrow$ Py + CH_3OH (route **X**) at low barrier, e.g., $\Delta G^{\ddagger}_{HT}$ = 6.0 kcal/mol calculated for the DHT-2H_2O model (see Table 1 for $\Delta G^{\ddagger}_{HT}$ values and Figure 3 for TSs). This low $\Delta G^{\ddagger}_{HT}$ value suggests that the slowest step from $CH_2(OH)_2$ to CH_3OH is in fact likely to be the dehydration of $CH_2(OH)_2$ to OCH_2. The rate constant for the dehydration of $CH_2(OH)_2$ to OCH_2 at ambient conditions[138,139] is ∼5 × 10^{-3} s^{-1} (obtained in the pH range 6.0−7.8) or equivalently the estimated free energy barrier $\Delta G^{\ddagger}_{dehyd}$ is ∼20 kcal/mol. Consequently, the effective rate constant for transformation of $CH_2(OH)_2$ to CH_3OH is that of $CH_2(OH)_2$ dehydration (for all three of our models; see Table 1 and Figure 3).[150]

In a fashion similar to the HCOOH reduction, the reduction of OCH_2 proceeds homogeneously via a *coupled* HTPT step, which we illustrate using structures determined via IRC calculations. Figure 5 shows the reactant complex R involving **PyH_2**, OCH_2, and H_2O for the DHT-1H_2O model. In this complex, the C of OCH_2 is still far from the hydridic H of **PyH_2** (e.g., R_{C-H} = 2.39 Å), and all moieties are approximately charge neutral (e.g., HT has not yet commenced, and all species have $q \sim 0$). At the TS, OCH_2 is in the process of accepting a hydride from **PyH_2**, and, importantly, there is no significant PT, as evidenced by the relatively large R_{O-H} = 1.73 Å value relative to the R_{O-H} value 0.98 Å of the product. Thus, the TS consists of HT character, again justifying our use of the experimental HT activation entropy factor proposed in Section 2.

As the reaction progresses energetically downhill from the TS toward the product, HT completes, transiently forming the methoxide (OCH_3^-) anion-type moiety, displayed in structure i of Figure 5. In analogy to the second HTPT step, the PT occurs well into the exit channel after the HT TS and involves no TS on the way to the reaction product. Thus, the HT and PT are *coupled* in this HTPT process. The PT aspect of the reaction involves a proton relay chain for the one and two H_2O DHT model cases. The newly formed methoxide anion-like moiety is negatively charged [$q(OCH_3^-)$ = −0.76e] and possesses a sufficiently basic carbonyl (pK_a of methanol is ∼16)[151] that it abstracts a proton from a neighboring hydrogen-bonded H_2O (structure ii) to initiate a proton relay cascade: a transient hydroxide anion-like moiety is produced (structure ii), which then abstracts an H^+ from PyH^+ (the oxidized **PyH_2** which has earlier resulted from HT) as CH_3OH formation is completed (structure iii) to finally form Py together with H_2O' and CH_3OH in the product complex, P. The HTPT activation free energies for the three cases are reported in Table 1. Our

dx.doi.org/10.1021/ja510131a | J. Am. Chem. Soc. XXXX, XXX, XXX−XXX

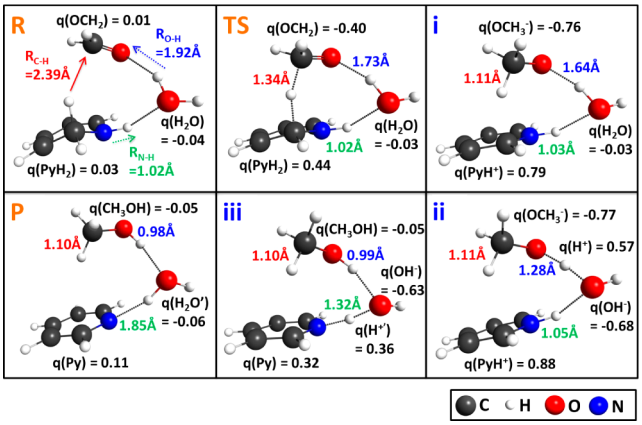

Figure 5. Reduction of formaldehyde by $\mathbf{PyH_2}$ to methanol (via the DHT-1H_2O model) in a coupled HTPT step. In the reactant complex R, all moieties ($\mathbf{PyH_2}$, OCH_2, and H_2O) are approximately neutral (e.g., $q \sim 0$, in electronic charge units, e) and the HT reaction from $\mathbf{PyH_2}$ to OCH_2 has not commenced (e.g., R_{C-H} = 2.39 Å). The reaction then proceeds to the TS, which is of HT character: OCH_2 becomes more negatively charged [$q(OCH_2) = -0.40e$] on the way to full HT, whereas $\mathbf{PyH_2}$ becomes more positive [$q(\mathbf{PyH_2}) = 0.44e$] without any significant PT (e.g., R_{O-H} = 1.73 Å). As the reaction progresses energetically downhill from the TS toward the product, the HT completes and methoxide anion (OCH_3^-) is formed in structure i. The basic methoxide [$q(OCH_3^-) = -0.77e$] now begins to abstract a proton from the neighboring H_2O in structure ii to form methanol (CH_3OH) in structure iii. The proton relay continues as the first PT-produced transient hydroxide anion-like OH^- now abstracts a proton from PyH^+ to finally form the product complex P of Py, CH_3OH, and H_2O', where ′ denotes the water molecule newly formed in the proton relay.

earlier remark about a minor activation entropy effect for the proton relay aspects of the second step also applies here.

It is noteworthy that HT from a related dihydropyridine species to an aldehyde has been observed.[152,153] In eq 2, 10-methyl-9,10-dihydroacidine transfers its hydride to benzaldehyde to form benzyl alcohol in the presence of perchloric acid ($HClO_4$), which acts as the H^+ donor.[152] The HTPT reaction between $\mathbf{PyH_2}$ and OCH_2 to form methanol (Scheme 8, route **X**) is analogous to eq 2; however, route **X** differs slightly because $\mathbf{PyH_2}$ acts as both the hydride and proton donor.

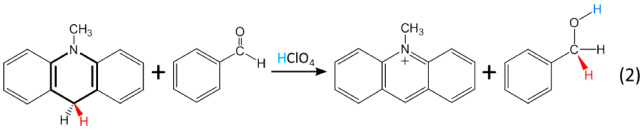

3.7. Commentary on the Homogeneous Mechanism for CO_2 Reduction to CH_3OH Catalyzed by Pyridine. The preceding results in this section allow us to map out a complete mechanism of Py-catalyzed CO_2 reduction to CH_3OH via three HTPT steps (Scheme 9), where the first HTPT to CO_2 is uncoupled and PT may be cathode-assisted and sequential and the final two HTPT steps are coupled in character and homogeneous. These results are summarized in Table 1 and Figure 3. Examination of Table 1 and Figure 3 shows that the second HTPT step, that of HCOOH reduction, is the highest HTPT free energy barrier step for the reduction of CO_2 to CH_3OH by $\mathbf{PyH_2}$ in all cases. However, in the DHT-2H_2O case, the second HTPT barrier $\Delta G^{\ddagger}_{HT}$ = 18.7 kcal/mol is lower than the methanediol dehydration barrier $\Delta G^{\ddagger}_{dehyd}$ of ∼20 kcal/mol (see Section 3.6 and Figure 3). In this connection, it is noteworthy that substrate and/or hydride donor activation[29,135,152,154] can act to further lower $\Delta G^{\ddagger}_{HT}$. For example, K^+ and PyH^+ in solution can activate the carbonyls for HT (see discussion at end of Section 3.4). However, even without this additional activation, the $\mathbf{PyH_2}$-catalyzed reduction of CO_2 to CH_3OH is kinetically facile. Moreover, we have found that for the second and third reduction steps, a proton relay chain can noticeably reduce the reaction barriers. However, even without these proton relays, Table 1, and the methanediol dehydration barrier $\Delta G^{\ddagger}_{dehyd}$ of ∼20 kcal/mol, these reactions remain viable in activation free energy terms.

For completeness, we have also considered a potential side reaction that might significantly impact the Faradaic yield for the overall $\mathbf{PyH_2}$-catalyzed CO_2 reduction to CH_3OH: HT from $\mathbf{PyH_2}$ to a proton donor such as PyH^+ to evolve H_2 ($\mathbf{PyH_2}$ + PyH^+ = PyH^+ + Py + H_2). We have calculated that this route

Scheme 9. Homogeneous Mechanism of Py-Catalyzed CO_2 Reduction to CH_3OH via PyH_2/Py HTPT Processes[a]

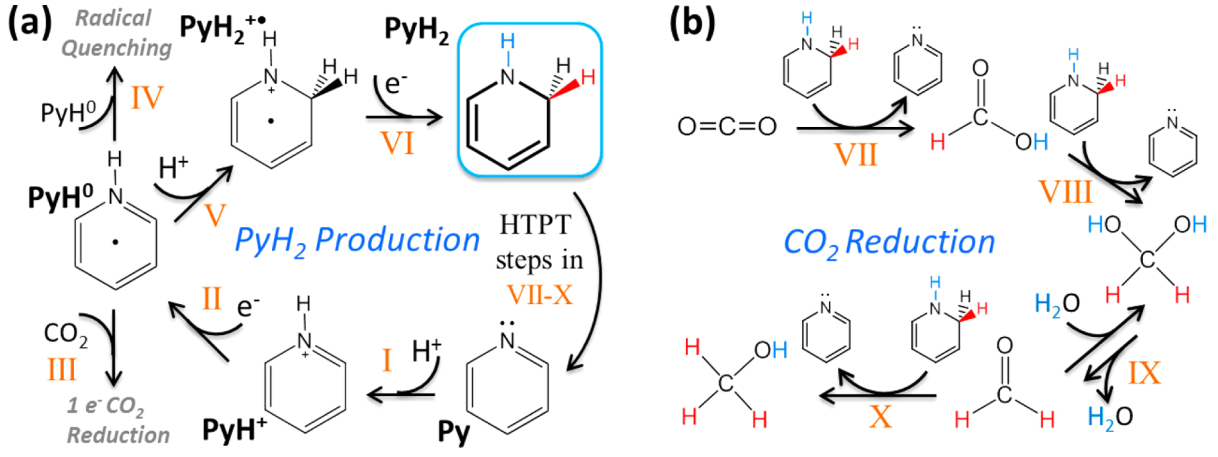

[a](a) $\mathbf{PyH_2}$ formation issues. In routes **I** and **II**,[46] Py accepts an H^+ to form PyH^+ and then an e^- to form the PyH^0 neutral radical, which then either reduces CO_2 by 1 e^- reduction to form $PyCOOH^0$ (route **III**)[46] or undergoes radical self-quenching (route **IV**) to produce H_2 + 2Py, a 4,4′ coupled dimer or Py + $\mathbf{PyH_2}$. Alternatively, and of most importance in the present work, in routes **V** and **VI**, PyH^0 accepts a second H^+ and then a second e^- to form the potent recyclable organo-hydride $\mathbf{PyH_2}$. (b) CO_2 reduction to methanol. In routes **VII**–**X**, the produced $\mathbf{PyH_2}$ participates in each of three catalytic HTPT steps to reduce CO_2 to CH_3OH and H_2O while recovering the Py catalyst.

dx.doi.org/10.1021/ja510131a | J. Am. Chem. Soc. XXXX, XXX, XXX−XXX

involves a $\Delta G^{\ddagger}_{HT}$ of 24.0 kcal/mol, which demonstrates that such unproductive heterolytic quenching to form H_2 is dominated by the **PyH$_2$**-catalyzed HT to CO_2, HCOOH, and OCH_2, as well as the methanediol dehydration. The higher barrier for H_2 production is supported by the fact that the HT reaction by the corresponding dihydropyridine species in eq 2 can be carried out under acidic conditions without appreciable H_2 production.[152] The very high (96%) Faradaic yield of the p-GaP system[23] is also consistent with the unfavorable heterolytic quenching to form H_2.

We recognize that homogeneous components of a pathway for a pyridine-mediated CO_2 reduction to CH_3OH have been argued to be ruled out in several recent theoretical studies,[80,92] and we briefly address this here. One key premise raised by the studies' authors is that 1e$^-$ reduction of PyH$^+$ to PyH^0 cannot occur at experimental conditions.[80] However, this statement is not supported by the fact that highly reducing electrons are present in both the photoelectrochemical p-GaP system (E_{CBM} ~ −1.5 V vs SCE at pH 5)[82,83] and the photochemical $[Ru(phen)_3]^{2+}$/ascorbate system[89] to populate PyH$^+$'s LUMO (E^0_{calc} ~ −1.3 V vs SCE) to form the solution-phase PyH^0 (see the discussion in Section 3.1). Another premise is that radical self-quenching will render PyH^0 inactive.[92] We have already pointed out in Section 3.1 that radical self-quenching of PyH^0 can actually yield the productive **PyH$_2$** via disproportionation.[105] In addition, it is relevant to note that Py-related neutral radicals of nicotinamide,[43] acridine,[44] and 3,6-diaminoacridine[45] have been experimentally observed and are key intermediate species en route to forming the related dihydropyridine species.

Finally, and in contrast to the present identification of **PyH$_2$** as the important catalytic agent in homogeneous and cathode-assisted Py-mediated CO_2 reduction, it has been suggested that a surface-adsorbed dihydropyridine might reduce CO_2 by HT from its N−H bond.[92,93] We already noted that a solution-phase dihydropyridine is normally involved in observed HT reactions such as those in eqs 1 and 2. In any event, in our view, the proposed reduction through the surface-adsorbed species does not provide a viable HT mechanism.[155] A key issue is that the adsorbed dihydropyridine's N−H bond is proposed to act as a hydride donor.[93] However, the N−H hydrogen is protic, not hydridic; this suggestion is not consistent with the considerable literature concerning HT from dihydropyridines,[29,39,40,42,75,121,122,124,125,127,152,153] including the present work, which uniformly shows that the hydride transfers from the hydridic hydrogen of the C−H bond and not from N−H.[156]

3.8. Recovery of Aromaticity Drives Hydride Transfer from PyH$_2$. We have shown that CO_2 reduction to CH_3OH is accomplished via three successive HTPT steps by **PyH$_2$**. We now describe the principle that makes **PyH$_2$** an effective HT agent. In fact, **PyH$_2$**'s strong hydride nucleophilicity could be regarded in a certain sense as rather surprising; it is an organohydride where the hydridic H is provided by a C−H bond. Consequently, **PyH$_2$** differs significantly from conventional transition-metal hydrides (M−H)[22,27,126,128] in that C is more electronegative than the transition metals (M), e.g., Co, Ni, and Pt. We suggest that the origin of the hydride nucleophilicity of the hydridic C−H bonds of **PyH$_2$** lies in the energetics of dearomatization and aromatization of PyH$^+$,[46] a concept similar to one applied to metal−ligand cooperation in catalysis involving transition-metal complexes.[157,158] During the formation of **PyH$_2$**, the first reduction of PyH$^+$ to PyH^0 dearomatizes PyH$^+$'s ring (Scheme 9a, route **II**), a destabilization consistent with PyH$^+$'s highly negative E^0 of ~−1.3 V vs SCE. PyH$^+$'s proclivity to regain its aromaticity drives HT from the hydridic C−H bond of **PyH$_2$** to the carbon atoms of CO_2, HCOOH, and OCH_2 to form reduced products and to recover the aromatic PyH$^+$ (or Py) catalyst. This mirrors the aromatization driving force several of us previously described in PyCOOH^0 formation via a 1e$^-$ process.[46]

Figure 6 confirms the dearomatization−aromatization principle by demonstrating that the free energy barrier for

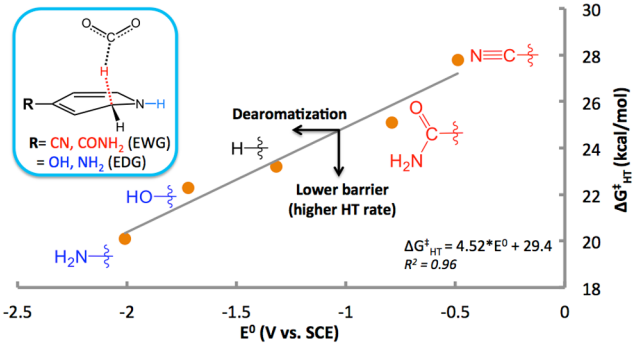

Figure 6. Calculated standard activation free energy barrier $\Delta G^{\ddagger}_{HT}$ (kcal/mol) to hydride transfer to CO_2 correlates linearly with the degree of dearomatization of the hydride donor. $\Delta G^{\ddagger}_{HT}$ (kcal/mol) is calculated for hydride transfer to CO_2 to form $HCOO^-$ using the DHT model of Figure 2a (also shown here in the inset). E^0 measures the energy required to dearomatize PyH$^+$ and related protonated aromatic amines and thus serves as a quantitative measure of the degree of dearomatization. E^0 (V vs SCE) is our calculated standard reduction potential for the protonated pyridine species indicated in Scheme 9a, route **II**, e.g., PyH$^+$ + e$^-$ = PyH^0 (see Supporting Information, Section 1b, for details of E^0 calculations). We substitute **PyH$_2$** with electron-withdrawing (R = CN, $CONH_2$) and electron-donating (R = OH, NH_2) groups in the para position of the ring to establish a wide range of E^0, spanning from −0.49 to −2.10 V vs SCE, and thus a broad degree of dearomatization.

HT to CO_2, $\Delta G^{\ddagger}_{HT}$, decreases with increasing cost of dearomatization, as measured by the standard reduction potential E^0 defined in Scheme 9a, route **II**. We obtain a wide range of E^0 spanning from −0.49 to −2.10 V vs SCE by substituting electron-withdrawing (e.g., CN, $CONH_2$) and electron-donating (e.g., OH, NH_2) groups at **PyH$_2$**'s para position. We contend that as the E^0 of an aromatic species becomes increasingly negative, more energy is required to dearomatize that species by populating its LUMO (a benzene-like π^* orbital);[159] thus, E^0 is a quantitative measure of the energetic cost of dearomatization. The linear trend established in Figure 6 has a firm physical basis: as E^0 becomes more negative, the driving force to recover aromaticity increases accordingly, which, in turn, results in lower $\Delta G^{\ddagger}_{HT}$ and consequently a higher hydride transfer rate. Figure 6 shows that the effect of dearomatization−aromatization on $\Delta G^{\ddagger}_{HT}$ enables **PyH$_2$** to act in its unique role as a potent hydride donor, which here is one that catalyzes the reduction of CO_2 to CH_3OH through three HTPT steps and which is regenerated through the **PyH$_2$**/Py redox couple (Scheme 9a, routes **I**, **II**, **V**, and **VI**).

4. CONCLUDING REMARKS

In summary, we have elucidated a kinetically and thermodynamically viable mechanism for the reduction of CO_2 to CH_3OH by 1,2-dihydropyridine, **PyH$_2$**, via primarily homoge-

dx.doi.org/10.1021/ja510131a | J. Am. Chem. Soc. XXXX, XXX, XXX−XXX

neous steps with some heterogeneous cathode assistance.[160] Our proposed sequential PT−ET−PT−ET process of alternating proton and electron transfers (Scheme 9a, routes **I**, **II**, **V**, and **VI**) that initially transforms Py into the catalytic species $\mathbf{PyH_2}$ is supported by the observation of a similar process occurring in Py-related species, e.g., nicotinamide and acridines,[43−45] where the aromatic PyH^+ is dearomatized during the process. Subsequently, driven by the proclivity to recover aromaticity, $\mathbf{PyH_2}$ transfers its hydridic hydrogen in three successive steps to CO_2, HCOOH, and OCH_2 to ultimately form CH_3OH (Scheme 9b, routes **VII**−**X**). The initial reduction of CO_2 is mediated by an uncoupled, sequential HTPT process; for the subsequent HCOOH and OCH_2 reductions, coupled HTPT occurs in which PT is mediated by a proton relay via one or two water molecules.

We stress that while we have theoretically demonstrated CO_2 reduction proceeding primarily homogeneously after $\mathbf{PyH_2}$ formation we do not rule out possible intrinsically surface-catalyzed events, most especially on a Pt electrode (see Section 3.1). On the other hand, we suggest that both Bocarsly's p-GaP[23] (modulo the two cathode-assisted aspects we have described within) and MacDonnell's surface-free Ru(II)/ascorbate[89] systems are homogeneous processes mediated by our proposed recyclable $\mathbf{PyH_2}$/Py redox couple. This suggestion is reinforced by Tanaka's demonstration that the related dihydropyridine ($\mathbf{Ru(bpy)_2(pbnH_2)^{2+}}$) species homogeneously reduces CO_2 to $HCOO^-$ by hydride transfer;[29] in addition, the related 10-methyl-9,10-dihydroacidine has been demonstrated to convert benzaldehyde into benzyl alcohol via a HTPT step.[152] We thus theoretically predict that pyridine's intriguing catalytic behavior lies in the fundamentally homogeneous HT chemistry of the $\mathbf{PyH_2}$/Py redox couple, whose production (Scheme 9a) is driven by a dearomatization−aromatization process, as argued in connection with Figure 6.

It is noteworthy that the $\mathbf{PyH_2}$/Py redox couple, by its hydride transfer to carbonyl for C−H bond formation, closely imitates the NADPH/$NADP^+$ catalyzed reduction step in photosynthesis (Scheme 5a). Our results thus suggest that the NADPH/$NADP^+$ couple is similar to the $\mathbf{PyH_2}$/Py couple in that dearomatization is used to store energy that is subsequently used to drive HT while regaining aromaticity. Finally, we propose that the advantage of the recyclable $\mathbf{PyH_2}$/Py redox couple extends beyond the mechanism of CO_2 reduction described within to provide inexpensive and green alternatives to commonly used hydride donors in organic synthesis.

■ ASSOCIATED CONTENT

Supporting Information

Computational methods; overestimation of activation entropies using ideal gas partition functions; thermodynamic quantities referenced to reactant complex; recovery of the pyridine catalyst from the 4,4′ coupled dimer; linearized Poisson−Boltzmann model of cation concentration near a biased cathode; reactivity of 1,2-dihydropyridine vs 1,4-dihydropyridine toward CO_2; hydride transfer from the N−H bond of 1,4-dihydropyridine; and coordinates of molecular structures. This material is available free of charge via the Internet at http://pubs.acs.org.

■ AUTHOR INFORMATION

Corresponding Author

charles.musgrave@colorado.edu

Notes

The authors declare no competing financial interest.

■ ACKNOWLEDGMENTS

This work was supported in part by NSF grant nos. CHE-1214131 (C.B.M. and A.M.H.) and CHE-1112564 (J.T.H.). We also gratefully acknowledge use of XSEDE supercomputing resources (NSF ACI-1053575) and the Janus supercomputer, which is supported by NSF (CNS-0821794) and the University of Colorado Boulder. We also thank Dr. Yong Yan of NREL for useful discussions.

■ REFERENCES

(1) Arakawa, H.; Aresta, M.; Armor, J. N.; Barteau, M. A.; Beckman, E. J.; Bell, A. T.; Bercaw, J. E.; Creutz, C.; Dinjus, E.; Dixon, D. A.; Domen, K.; DuBois, D. L.; Eckert, J.; Fujita, E.; Gibson, D. H.; Goddard, W. A.; Goodman, D. W.; Keller, J.; Kubas, G. J.; Kung, H. H.; Lyons, J. E.; Manzer, L. E.; Marks, T. J.; Morokuma, K.; Nicholas, K. M.; Periana, R.; Que, L.; Rostrup-Nielson, J.; Sachtler, W. M. H.; Schmidt, L. D.; Sen, A.; Somorjai, G. A.; Stair, P. C.; Stults, B. R.; Tumas, W. *Chem. Rev.* **2001**, *101*, 953.

(2) Beckman, E. J. *Ind. Eng. Chem. Res.* **2003**, *42*, 1598.

(3) Benson, E. E.; Kubiak, C. P.; Sathrum, A. J.; Smieja, J. M. *Chem. Soc. Rev.* **2009**, *38*, 89.

(4) Cokoja, M.; Bruckmeier, C.; Rieger, B.; Herrmann, W. A.; Kühn, F. E. *Angew. Chem., Int. Ed.* **2011**, *50*, 8510.

(5) Darensbourg, D. J. *Inorg. Chem.* **2010**, *49*, 10765.

(6) Ganesh, I. *Curr. Sci.* **2011**, *101*, 731.

(7) Jiang, Z.; Xiao, T.; Kuznetsov, V. L.; Edwards, P. P. *Philos. Trans. R. Soc., A* **2010**, *368*, 3343.

(8) Mikkelsen, M.; Jorgensen, M.; Krebs, F. C. *Energy Environ. Sci.* **2010**, *3*, 43.

(9) Olah, G. A.; Goeppert, A.; Prakash, G. K. S. *J. Org. Chem.* **2009**, *74*, 487.

(10) Olah, G. A.; Prakash, G. K. S.; Goeppert, A. *J. Am. Chem. Soc.* **2011**, *133*, 12881.

(11) Morris, A. J.; Meyer, G. J.; Fujita, E. *Acc. Chem. Res.* **2009**, *42*, 1983.

(12) Hull, J. F.; Himeda, Y.; Wang, W.-H.; Hashiguchi, B.; Periana, R.; Szalda, D. J.; Muckerman, J. T.; Fujita, E. *Nat. Chem.* **2012**, *4*, 383.

(13) Doherty, M. D.; Grills, D. C.; Muckerman, J. T.; Polyansky, D. E.; Fujita, E. *Coord. Chem. Rev.* **2010**, *254*, 2472.

(14) Kumar, B.; Llorente, M.; Froehlich, J.; Dang, T.; Sathrum, A.; Kubiak, C. P. *Annu. Rev. Phys. Chem.* **2012**, *63*, 541.

(15) Alstrum-Acevedo, J. H.; Brennaman, M. K.; Meyer, T. J. *Inorg. Chem.* **2005**, *44*, 6802.

(16) Chen, Z.; Glasson, C. R. K.; Holland, P. L.; Meyer, T. J. *Phys. Chem. Chem. Phys.* **2013**, *15*, 9503.

(17) Kang, P.; Meyer, T. J.; Brookhart, M. *Chem. Sci.* **2013**, *4*, 3497.

(18) Costentin, C.; Robert, M.; Savéant, J.-M. *Chem. Soc. Rev.* **2013**, *42*, 2423.

(19) Gennaro, A.; Isse, A. A.; Savéant, J. M.; Severin, M. G.; Vianello, E. *J. Am. Chem. Soc.* **1996**, *118*, 7190.

(20) Savéant, J.-M. *Chem. Rev.* **2008**, *108*, 2348.

(21) Ashley, A. E.; Thompson, A. L.; O'Hare, D. *Angew. Chem., Int. Ed.* **2009**, *48*, 9839.

(22) Balaraman, E.; Gunanathan, C.; Zhang, J.; Shimon, L. J. W.; Milstein, D. *Nat. Chem.* **2011**, *3*, 609.

(23) Barton, E. E.; Rampulla, D. M.; Bocarsly, A. B. *J. Am. Chem. Soc.* **2008**, *130*, 6342.

(24) Chakraborty, S.; Zhang, J.; Krause, J. A.; Guan, H. *J. Am. Chem. Soc.* **2010**, *132*, 8872.

(25) Huang, F.; Lu, G.; Zhao, L. L.; Li, H. X.; Wang, Z. X. *J. Am. Chem. Soc.* **2010**, *132*, 12388.

(26) Huang, K.-W.; Han, J. H.; Musgrave, C. B.; Fujita, E. *Organometallics* **2006**, *26*, 508.
(27) Jeletic, M. S.; Mock, M. T.; Appel, A. M.; Linehan, J. C. *J. Am. Chem. Soc.* **2013**, *135*, 11533.
(28) Menard, G.; Stephan, D. W. *J. Am. Chem. Soc.* **2010**, *132*, 1796.
(29) Ohtsu, H.; Tanaka, K. *Angew. Chem., Int. Ed.* **2012**, *51*, 9792.
(30) Dubois, M. R.; Dubois, D. L. *Acc. Chem. Res.* **2009**, *42*, 1974.
(31) Riduan, S. N.; Zhang, Y. G.; Ying, J. Y. *Angew. Chem., Int. Ed.* **2009**, *48*, 3322.
(32) Seshadri, G.; Lin, C.; Bocarsly, A. B. *J. Electroanal. Chem.* **1994**, *372*, 145.
(33) Cole, E. B.; Lakkaraju, P. S.; Rampulla, D. M.; Morris, A. J.; Abelev, E.; Bocarsly, A. B. *J. Am. Chem. Soc.* **2010**, *132*, 11539.
(34) Canfield, D.; Frese, K. W. *J. Electrochem. Soc.* **1983**, *130*, 1772.
(35) Frese, K. W.; Canfield, D. *J. Electrochem. Soc.* **1984**, *131*, 2518.
(36) Zimmerman, P. M.; Paul, A.; Zhang, Z. Y.; Musgrave, C. B. *Angew. Chem., Int. Ed.* **2009**, *48*, 2201.
(37) Zimmerman, P. M.; Zhang, Z. Y.; Musgrave, C. B. *Inorg. Chem.* **2010**, *49*, 8724.
(38) Lim, C.-H.; Holder, A. M.; Hynes, J. T.; Musgrave, C. B. *Inorg. Chem.* **2013**, *52*, 10062.
(39) Eisner, U.; Kuthan, J. *Chem. Rev.* **1972**, *72*, 1.
(40) McSkimming, A.; Colbran, S. B. *Chem. Soc. Rev.* **2013**, *42*, 5439.
(41) Connon, S. J. *Org. Biomol. Chem.* **2007**, *5*, 3407.
(42) Chen, Q.-A.; Chen, M.-W.; Yu, C.-B.; Shi, L.; Wang, D.-S.; Yang, Y.; Zhou, Y.-G. *J. Am. Chem. Soc.* **2011**, *133*, 16432.
(43) Schmakel, C. O.; Santhanam, K. S. V.; Elving, P. J. *J. Electrochem. Soc.* **1974**, *121*, 345.
(44) Kaye, R. C.; Stonehill, H. I. *J. Chem. Soc.* **1951**, 27.
(45) Fujii, S.; Tatsumoto, N.; Yamaoka, K. *J. Electroanal. Chem. Interfacial Electrochem.* **1988**, *244*, 235.
(46) Lim, C.-H.; Holder, A. M.; Musgrave, C. B. *J. Am. Chem. Soc.* **2012**, *135*, 142.
(47) Zhao, Y.; Truhlar, D. *Theor. Chem. Acc.* **2008**, *120*, 215.
(48) Harihara, Pc; Pople, J. A. *Theor. Chim. Acta.* **1973**, *28*, 213.
(49) Binkley, J. S.; Pople, J. A. *Int. J. Quantum Chem.* **1975**, *9*, 229.
(50) Dunning, T. H. *J. Chem. Phys.* **1989**, *90*, 1007.
(51) Li, H.; Jensen, J. H. *J. Comput. Chem.* **2004**, *25*, 1449.
(52) Li, H.; Pomelli, C. S.; Jensen, J. H. *Theor. Chem. Acc.* **2003**, *109*, 71.
(53) Bianco, R.; Hay, P. J.; Hynes, J. T. *J. Phys. Chem. A* **2011**, *115*, 8003.
(54) Kang, J. K.; Musgrave, C. B. *J. Chem. Phys.* **2002**, *116*, 275.
(55) Koch, D. M.; Toubin, C.; Peslherbe, G. H.; Hynes, J. T. *J. Phys. Chem. C* **2008**, *112*, 2972.
(56) Somani, S.; Mukhopadhyay, A.; Musgrave, C. *J. Phys. Chem. C* **2011**, *115*, 11507.
(57) Bianco, R.; Hay, P. J.; Hynes, J. T. *Energy Environ. Sci.* **2012**, *5*, 7741.
(58) Stirling, A. s.; Pápai, I. *J. Phys. Chem. B* **2010**, *114*, 16854.
(59) Wang, B.; Cao, Z. *J. Comput. Chem.* **2013**, *34*, 372.
(60) Barton, B. E.; Olsen, M. T.; Rauchfuss, T. B. *J. Am. Chem. Soc.* **2008**, *130*, 16834.
(61) Fetter, J. R.; Qian, J.; Shapleigh, J.; Thomas, J. W.; García-Horsman, A.; Schmidt, E.; Hosler, J.; Babcock, G. T.; Gennis, R. B.; Ferguson-Miller, S. *Proc. Natl. Acad. Sci. U.S.A.* **1995**, *92*, 1604.
(62) Lutz, S.; Tubert-Brohman, I.; Yang, Y.; Meuwly, M. *J. Biol. Chem.* **2011**, *286*, 23679.
(63) Bonin, J.; Costentin, C.; Robert, M.; Savéant, J.-M.; Tard, C. *Acc. Chem. Res.* **2011**, *45*, 372.
(64) DuBois, D. L.; Bullock, R. M. *Eur. J. Inorg. Chem.* **2011**, 1017.
(65) Bianco, R.; Hynes, J. T. *J. Phys. Chem. A* **1999**, *103*, 3797.
(66) Huynh, M. H. V.; Meyer, T. J. *Chem. Rev.* **2007**, *107*, 5004.
(67) Benson, S. W. *The Foundations of Chemical Kinetics*; McGraw-Hill: New York, 1960.
(68) Qu, S.; Dang, Y.; Song, C.; Wen, M.; Huang, K.-W.; Wang, Z.-X. *J. Am. Chem. Soc.* **2014**, *136*, 4974.
(69) Liang, Y.; Liu, S.; Xia, Y.; Li, Y.; Yu, Z.-X. *Chem.—Eur. J.* **2008**, *14*, 4361.
(70) Huang, D.; Makhlynets, O. V.; Tan, L. L.; Lee, S. C.; Rybak-Akimova, E. V.; Holm, R. H. *Inorg. Chem.* **2011**, *50*, 10070.
(71) Huang, D.; Makhlynets, O. V.; Tan, L. L.; Lee, S. C.; Rybak-Akimova, E. V.; Holm, R. H. *Proc. Natl. Acad. Sci. U.S.A.* **2011**, *108*, 1222.
(72) Martin, R. L.; Hay, P. J.; Pratt, L. R. *J. Phys. Chem. A* **1998**, *102*, 3565.
(73) Wen, M.; Huang, F.; Lu, G.; Wang, Z.-X. *Inorg. Chem.* **2013**, *52*, 12098.
(74) Strajbl, M.; Sham, Y. Y.; Villà, J.; Chu, Z. T.; Warshel, A. *J. Phys. Chem. B* **2000**, *104*, 4578.
(75) Srinivasan, R.; Medary, R. T.; Fisher, H. F.; Norris, D. J.; Stewart, R. *J. Am. Chem. Soc.* **1982**, *104*, 807.
(76) Tanaka, R.; Yamashita, M.; Chung, L. W.; Morokuma, K.; Nozaki, K. *Organometallics* **2011**, *30*, 6742.
(77) *Gaussian 09*, Revision A.1; see Supporting Information for full reference.
(78) Schmidt, M. W.; Baldridge, K. K.; Boatz, J. A.; Elbert, S. T.; Gordon, M. S.; Jensen, J. H.; Koseki, S.; Matsunaga, N.; Nguyen, K. A.; Su, S. J.; Windus, T. L.; Dupuis, M.; Montgomery, J. A. *J. Comput. Chem.* **1993**, *14*, 1347.
(79) Tossell, J. A. *Comput. Theor. Chem.* **2011**, *977*, 123.
(80) Keith, J. A.; Carter, E. A. *J. Am. Chem. Soc.* **2012**, *134*, 7580.
(81) This contrasts with a recent theoretical estimate (ref 93) of the conduction band minimum (E_{CBM}) of p-GaP of −0.9 V vs SCE, which is significantly below the observed E_{CBM} of −1.5 V vs SCE. This estimate led the authors to conclude that homogeneous PyH^0 species cannot be formed in the p-GaP electrode system.
(82) Gratzel, M. *Nature* **2001**, *414*, 338.
(83) Walter, M. G.; Warren, E. L.; McKone, J. R.; Boettcher, S. W.; Mi, Q.; Santori, E. A.; Lewis, N. S. *Chem. Rev.* **2010**, *110*, 6446.
(84) Beranek, R. *Adv. Phys. Chem.* **2011**, *2011*, 786759.
(85) The reported p-GaP conduction band minimum, E_{CBM}, is ∼−1.0 V vs NHE at pH 1. Correcting for the SCE reference potential shifts the band edge by −0.24 V from NHE. At the same time, the band edge shifts to more cathodic potentials with increasing pH by −0.059 V/pH at 298 K (ref 84).
(86) Lebègue, E.; Agullo, J.; Morin, M.; Bélanger, D. *ChemElectroChem* **2014**, *1*, 1013.
(87) An anonymous reviewer of an earlier version of this manuscript suggested the importance of examination of CO_2 reduction with pyridine under acidic conditions with a carbon electrode. In connection with an experiment very recently reported (ref 86), it was suggested that PyH^0 was produced with a glassy carbon electrode, and a catalytic current was observed in the presence of CO_2. Further detailed results for this system will be of considerable interest in connection with the present work.
(88) Xiang, D.; Magana, D.; Dyer, R. B. *J. Am. Chem. Soc.* **2014**, *136*, 14007.
(89) Boston, D. J.; Xu, C.; Armstrong, D. W.; MacDonnell, F. M. *J. Am. Chem. Soc.* **2013**, *135*, 16252.
(90) In ref 89, after 6 h of photochemical reduction of CO_2 catalyzed by pyridine, formate was produced at relatively high yield (18 mM), but methanol was produced at low yield (66 μM). The issue of formate formation is discussed in Section 3.5.
(91) Boston, D. J.; Pachón, Y. M. F.; Lezna, R. O.; de Tacconi, N. R.; MacDonnell, F. M. *Inorg. Chem.* **2014**, *53*, 6544.
(92) Keith, J. A.; Carter, E. A. *Chem. Sci.* **2013**, *4*, 1490.
(93) Keith, J. A.; Carter, E. A. *J. Phys. Chem. Lett.* **2013**, *4*, 4058.
(94) Costentin, C.; Canales, J. C.; Haddou, B.; Savéant, J.-M. *J. Am. Chem. Soc.* **2013**, *135*, 17671.
(95) Ertem, M. Z.; Konezny, S. J.; Araujo, C. M.; Batista, V. S. *J. Phys. Chem. Lett.* **2013**, 745.
(96) Yan, Y.; Zeitler, E. L.; Gu, J.; Hu, Y.; Bocarsly, A. B. *J. Am. Chem. Soc.* **2013**, *135*, 14020.
(97) Yasukouchi, K.; Taniguchi, I.; Yamaguchi, H.; Shiraishi, M. *J. Electroanal. Chem. Interfacial Electrochem.* **1979**, *105*, 403.

(98) Portenkirchner, E.; Enengl, C.; Enengl, S.; Hinterberger, G.; Schlager, S.; Apaydin, D.; Neugebauer, H.; Knör, G.; Sariciftci, N. S. *ChemElectroChem.* **2014**, *1*, 1543.
(99) The loss of PyH^0's aromaticity is unfortunately not conveyed in the molecular structure of Scheme 2.
(100) Morris, A. J.; McGibbon, R. T.; Bocarsly, A. B. *ChemSusChem* **2011**, *4*, 191.
(101) Kamrath, M. Z.; Relph, R. A.; Johnson, M. A. *J. Am. Chem. Soc.* **2010**, *132*, 15508.
(102) This result contrasts the proposal that PyH^0 is not reactive due to its high pK_a of ∼27 (ref 80). We calculated a similarly high pK_a of ∼31 (ref 46). However, we argued that a pK_a analysis applies only to reactions occurring via the sequence of PT then ET, which is irrelevant for PyH^0's reaction with CO_2 that occurs via the sequence of first ET followed by PT (ref 46).
(103) Leuschner, R.; Krohn, H.; Dohrmann, J. K. *Ber. Bunsen-Ges.* **1984**, *88*, 462.
(104) Raghavan, R.; Iwamoto, R. T. *J. Electroanal. Chem. Interfacial Electrochem.* **1978**, *92*, 101.
(105) Kikuchi, K.; Koizumi, M. *B Chem. Soc. Jpn.* **1967**, *40*, 736.
(106) A similar process has been observed (ref 105) for the quenching of two 3,6-diaminoacridinium radicals to form the corresponding dihydropyridine species (3,6-diaminoacridane) and 3,6-diaminoacridine.
(107) Rose, M. C.; Stuehr, J. *J. Am. Chem. Soc.* **1968**, *90*, 7205.
(108) The rate constant for PyH^0 quenching is $\sim 10^9$ M^{-1} s^{-1} (ref 103). On the other hand, the rate constant for protonation/deprotonation ranges from 10^4 to 10^9 M^{-1} s^{-1} (ref 107) depending on pK_a differences between the donor and acceptor and other factors. Given that [HA] ≫ [PyH^0], it is likely that PyH_2 production via PT-ET to PyH^0 dominates over radical self-quenching.
(109) PyH^0 is predominantly protonated at its C_2 carbon (pK_a = 4.1) over that at its C_3 (pK_a = 0.2) and C_4 (pK_a = 2.4) positions; see Supporting Information, Section 1b for details.
(110) Protonation of related pyridine neutral radical species has been observed, e.g., the pK_a to protonate the C_9 position of 3,6-bis(dimethylamino) acridinium radical was determined to be 5.1 in aqueous solution (ref 111).
(111) Vogelmann, E.; Rauscher, W.; Krameer, H. E. A. *Photochem. Photobiol.* **1979**, *29*, 771.
(112) Vlachy, V. *Annu. Rev. Phys. Chem.* **1999**, *50*, 145.
(113) Bu, W.; Vaknin, D.; Travesset, A. *Langmuir* **2006**, *22*, 5673.
(114) Hunter, R. J. *Zeta Potential in Colloid Science: Principles and Applications*; Academic press: London, 1981; Vol. *8*.
(115) Angulo, M.; Montoya, M. R.; Galvin, R. M.; Mellado, J. M. R. *Electroanalysis* **1997**, *9*, 345.
(116) Hapiot, P.; Moiroux, J.; Saveant, J. M. *J. Am. Chem. Soc.* **1990**, *112*, 1337.
(117) Johnston, C. C.; Gardner, J. L.; Suelter, C. H.; Metzler, D. E. *Biochemistry* **1963**, *2*, 689.
(118) Shinkai, S.; Hamada, H.; Kusano, Y.; Manabe, O. *J. Chem. Soc., Perkin Trans. 2* **1979**, 699.
(119) Calvin, M. *Science* **1962**, *135*, 879.
(120) Raines, C. *Photosynth. Res.* **2003**, *75*, 1.
(121) Koizumi, T.-a.; Tanaka, K. *Angew. Chem., Int. Ed.* **2005**, *44*, 5891.
(122) Chen, Q.-A.; Gao, K.; Duan, Y.; Ye, Z.-S.; Shi, L.; Yang, Y.; Zhou, Y.-G. *J. Am. Chem. Soc.* **2012**, *134*, 2442.
(123) The proposed sequential PT-ET-PT-ET steps for **Ru(bpy)$_2$(pbnH$_2$)$^{2+}$** formation are consistent with the production of dihydropyridine species for the related nicotinamide and acridines (refs 43−45). More importantly, this is analogous to **PyH$_2$** formation, thus corroborating the viability of Schemes 2 and 4's routes I, II, V, and VI.
(124) Horn, M.; Schappele, L. H.; Lang-Wittkowski, G.; Mayr, H.; Ofial, A. R. *Chem.—Eur. J.* **2013**, *19*, 249.
(125) Richter, D.; Mayr, H. *Angew. Chem., Int. Ed.* **2009**, *48*, 1958.
(126) DuBois, D. L.; Berning, D. E. *Appl. Organomet. Chem.* **2000**, *14*, 860.
(127) Ellis, W. W.; Raebiger, J. W.; Curtis, C. J.; Bruno, J. W.; DuBois, D. L. *J. Am. Chem. Soc.* **2004**, *126*, 2738.
(128) Muckerman, J. T.; Achord, P.; Creutz, C.; Polyansky, D. E.; Fujita, E. *Proc. Natl. Acad. Sci. U.S.A.* **2012**, *109*, 15657.
(129) The *N* values of 1,4-cyclohexadiene, 10-methyl-9,10-dihydroacridine, and Hantzsch's ester were tabulated for HT in dichloromethane solvent, whereas DMSO was the solvent for $NaBH_4$. In contrast, our calculations on $PhenH_2$ and PyH_2 were performed with CPCM-modeled aqueous solvent. It has been experimentally observed (ref 124) that the *N* value is slightly greater when a more polar solvent is used (e.g., water).
(130) The linear dependence of $\Delta G^{\ddagger}_{HT}$ on *N* is implied from Mayr et al.'s log $k(20\ ^\circ C) = s(N + E)$ equation (defined in Figure 1), where the logarithm of the rate constant depends linearly on $\Delta G^{\ddagger}_{HT}$ that is linearly related to *N*.
(131) Because aqueous solution is considered for the reduction reactions, the possibility that PyH_2 is destroyed via HT to the water solvent ($PyH_2 + H_2O = PyH^+ + OH^- + H_2$) requires consideration. In Section 3.7, we discount the PyH_2 destruction route via HT to PyH^+ (the dominant cation acid in the solution) to form H_2 ($PyH_2 + PyH^+ = PyH^+ + Py + H_2$), with a calculated free energy barrier 24.0 kcal/mol. Because water (pK_a = 15.7) is a very much weaker acid than PyH^+ (pK_a = 5.3), PyH_2 HT to water will have a much higher barrier than does HT to PyH^+, and, at the same time, it will be even more thermodynamically unfavorable.
(132) Although PyH^+ is depicted as the sole proton donor in Scheme 6, any H_3O^+ present can also certainly protonate $HCOO^-$ to form HCOOH.
(133) Kamerlin, S. C. L.; Haranczyk, M.; Warshel, A. *ChemPhysChem* **2009**, *10*, 1125.
(134) As was the case for HT from ammonia borane (ref 38), no prebending of CO_2 is found to precede the TS.
(135) Proust-De Martin, F.; Dumas, R.; Field, M. J. *J. Am. Chem. Soc.* **2000**, *122*, 7688.
(136) Yoshioka, Y.; Schaefer, H. F.; Jordan, K. D. *J. Chem. Phys.* **1981**, *75*, 1040.
(137) Valadbeigi, Y.; Farrokhpour, H. *Int. J. Quantum Chem.* **2013**, *113*, 1717.
(138) Winkelman, J. G. M.; Ottens, M.; Beenackers, A. A. C. M. *Chem. Eng. Sci.* **2000**, *55*, 2065.
(139) Bell, R. P.; Evans, P. G. *Proc. R. Soc. London, Ser. A* **1966**, *291*, 297.
(140) Spackman, M. A. *J. Comput. Chem.* **1996**, *17*, 1.
(141) Beno, B. R.; Houk, K. N.; Singleton, D. A. *J. Am. Chem. Soc.* **1996**, *118*, 9984.
(142) Labet, V.; Morell, C.; Toro-Labbe, A.; Grand, A. *Phys. Chem. Chem. Phys.* **2010**, *12*, 4142.
(143) Bekele, T.; Christian, C. F.; Lipton, M. A.; Singleton, D. A. *J. Am. Chem. Soc.* **2005**, *127*, 9216.
(144) Williams, A. *Concerted Organic and Bio-Organic Mechanisms*; CRC Press: Boca Raton, FL, 1999.
(145) Black, K.; Liu, P.; Xu, L.; Doubleday, C.; Houk, K. N. *Proc. Natl. Acad. Sci. U.S.A.* **2012**, *109*, 12860.
(146) This sentence defines what we mean by coupled. In other language sometimes used (refs 141−145), the HTPT process could be termed concerted asynchronous. However, the definitions of the terms concerted and asynchronous are sometimes defined/interpreted differently (refs 141−145), so we do not insist on this usage.
(147) Barnes, D.; Zuman, P. *J. Electroanal. Chem. Interfacial Electrochem.* **1973**, *46*, 323.
(148) Norkus, E.; Pauliukaite, R.; Vaskelis, A.; Butkus, E.; Jusys, Z.; Kreneviciene, M. *J. Chem. Res., Synop.* **1998**, 320.
(149) Russell, P. G.; Kovac, N.; Srinivasan, S.; Steinberg, M. *J. Electrochem. Soc.* **1977**, *124*, 1329.
(150) The possible destruction of methanediol via HT from PyH_2 to produce the diolate negative ion, H_2, and PyH^+ can be neglected due to the diol's high pK_a value of ∼13 (refs 147 and 148), along the lines of the argument for the unimportance of HT from PyH_2 to H_2O in ref 131. We thank Prof. Matt Kanan (Stanford) for raising this issue.

(151) Ballinger, P.; Long, F. A. *J. Am. Chem. Soc.* **1960**, *82*, 795.
(152) Fukuzumi, S.; Ishikawa, M.; Tanaka, T. *Tetrahedron* **1986**, *42*, 1021.
(153) Kellogg, R. M. In *Comprehensive Organic Synthesis*; Trost, B. M., Fleming, I., Eds.; Pergamon: Oxford, 1991; p 79.
(154) Dumas, R.; Biou, V.; Halgand, F.; Douce, R.; Duggleby, R. G. *Acc. Chem. Res.* **2001**, *34*, 399.
(155) It was suggested that (ref 93) a surface hydride can be formed on a GaP surface, which is then transferred to the N of an adsorbed Py to form a surface-adsorbed dihydropyridine (assuming PT occurs from the solution phase). However, this proposal does not explain the observed catalytic role of Py: if GaP is capable of producing a hydride, then this hydride can directly transfer to CO_2, thus eliminating the role of Py as a HT mediator.
(156) In Supporting Information, Section 7, we calculate a ΔG^0_{rxn} of ~60 kcal/mol for the HT proposed in ref 93 from the N−H bond of 1,4-dihydropyridine to CO_2 to form $HCOO^-$. In addition, binding of 1,4-dihydropyridine to a surface Lewis acid site through the N lone pair, as proposed in ref 93, causes the N−H bond to be an even weaker hydride donor with a ΔG^0_{rxn} larger than the already high 60 kcal/mol for free 1,4-dihydropyridine. Thus, HT from the N−H bond of either a solution phase or surface-adsorbed dihydropyridine is highly endergonic and so is highly unlikely.
(157) Gunanathan, C.; Milstein, D. *Acc. Chem. Res.* **2011**, *44*, 588.
(158) Milstein, D. *Top. Catal.* **2010**, *53*, 915.
(159) Cyranski, M. K. *Chem. Rev.* **2005**, *105*, 3773.
(160) No surface reaction is invoked in our development, but we argue that the electrical double layer near the cathode plays the important role of assisting protonation in both the protonation of PyH^0 (Section 3.2) en route to $\mathbf{PyH_2}$ and of formate anion (Section 3.4).

dx.doi.org/10.1021/ja510131a | *J. Am. Chem. Soc.* XXXX, XXX, XXX−XXX